

1 **The bovine alveolar macrophage DNA methylome is resilient to infection with**
2 ***Mycobacterium bovis***

3 Running Title: Impact of mycobacterial infection on DNA methylation

4 Alan Mark O'Doherty ^{1,*}, Kevin Rue-Albrecht ^{2,*}, David Andrew Magee ¹, Simone Ahting ³,
5 Rachelle Elizabeth Irwin ⁴, Thomas Johnathan Hall ¹, John Arthur Browne ¹, Nicolas Claude
6 Nalpas ⁵, Colum Patrick Walsh ⁴, Stephen Vincent Gordon ^{6,7}, Marcin Wlodzimierz
7 Wojewodzic ⁸ and David Evan MacHugh ^{1,7}

8 ¹ Animal Genomics Laboratory, UCD School of Agriculture and Food Science, University
9 College Dublin, Belfield, Dublin, D04 V1W8, Ireland.

10 ² Kennedy Institute of Rheumatology, Nuffield Department of Orthopaedics, Rheumatology
11 and Musculoskeletal Sciences, University of Oxford, Headington, Oxford OX3 7FY, UK.

12 ³ Institute of Molecular Medicine, Trinity College Dublin, Dublin, D08 W9RT, Ireland.

13 ⁴ Genomic Medicine Research Group, Biomedical Sciences Research Institute, Centre for
14 Molecular Biosciences, University of Ulster, Coleraine, BT52 1SA UK.

15 ⁵ Quantitative Proteomics and Proteome Centre Tübingen, Interfaculty Institute for Cell
16 Biology, University of Tübingen, 72076 Tübingen, Germany.

17 ⁶ UCD School of Veterinary Medicine, University College Dublin, Belfield, Dublin, D04
18 V1W8, Ireland.

19 ⁷ UCD Conway Institute of Biomolecular and Biomedical Research, University College
20 Dublin, Belfield, Dublin, D04 V1W8, Ireland.

21 ⁸ University of Birmingham, School of Biosciences, Edgbaston, Birmingham, B15 2TT, UK.

22 ¶ These authors contributed equally to this work.

23 * Corresponding author: alan.odoherty@ucd.ie

24 **Grant Support:**

25 The study was supported by Science Foundation Ireland (SFI) Investigator Programme
26 Awards (grant nos. SFI/08/IN.1/B2038 and SFI/15/IA/3154), an SFI Technology Innovation
27 Development Award (grant no. 13/TIDA/B2675), a European Union Framework 7 Project
28 Grant (No: KBBE-211602-MACROSYS), and the UCD Wellcome Trust funded
29 Computational Infection Biology PhD Programme (Grant no: 097429/Z/11/Z).

30 **Keywords:** tuberculosis, DNA methylation, whole genome bisulfite sequencing, WGBS,
31 *Mycobacterium bovis*

32

33

34

35

36

37

38

39

40 **Abstract**

41 DNA methylation is pivotal in orchestrating gene expression patterns in various mammalian
42 biological processes. Perturbation of the bovine alveolar macrophage (bAM) transcriptome, due
43 to *Mycobacterium bovis* (*M. bovis*) infection, has been well documented; however, the impact of
44 this intracellular pathogen on the bAM epigenome has not been determined. Here, whole genome
45 bisulfite sequencing (WGBS) was used to assess the effect of *M. bovis* infection on the bAM
46 DNA methylome. The methylomes of bAM infected with *M. bovis* were compared to those of
47 non-infected bAM 24 hours post-infection (hpi). No differences in DNA methylation (CpG or
48 non-CpG) were observed. Analysis of DNA methylation at proximal promoter regions uncovered
49 >250 genes harbouring intermediately methylated (IM) promoters (average methylation of 33–
50 66%). Gene ontology analysis, focusing on genes with low, intermediate or highly methylated
51 promoters, revealed that genes with IM promoters were enriched for immune-related GO
52 categories; this enrichment was not observed for genes in the high or low methylation groups.
53 Targeted analysis of genes in the IM category confirmed the WGBS observation. This study is
54 the first in cattle examining genome-wide DNA methylation at single nucleotide resolution in an
55 important bovine cellular host-pathogen interaction model, providing evidence for IM promoter
56 methylation in bAM.

57

58 **Introduction**

59 Infection with *Mycobacterium bovis*, the causative agent of bovine tuberculosis (BTB),
60 accounts annually for more than \$3 billion of losses to global agriculture through lost
61 productivity and disease control costs¹. There is also evidence suggesting that the burden of
62 *M. bovis* as the cause of zoonotic tuberculosis in humans may be underestimated², which
63 highlights the need for a more detailed understanding of the impact of *M. bovis* in both cattle and
64 humans. Unravelling host cellular processes that are perturbed or manipulated by intracellular
65 pathogens is an important area of research in infection biology, particularly for disease control
66 and the development of next-generation diagnostics and prognostics. In this regard, host cell
67 epigenetic modifications induced, either as a component of the response to *M. bovis* infection, or
68 as an immunoevasion strategy by the pathogen itself, remain to be fully elucidated³.

69 Modifications to the genome, such as DNA methylation and histone tail modifications, in
70 combination with RNA-mediated regulatory mechanisms are fundamental in modulating tissue-
71 specific gene expression⁴⁻⁶. Epigenetic gene regulation represents an important framework for
72 understanding how environmental stimuli are disseminated to the transcriptome and preserved
73 through subsequent somatic cell divisions⁵. DNA methylation (5-methylcytosine), the most
74 widely studied genome modification, is involved in a variety of cellular processes including
75 genomic imprinting, X-chromosome inactivation, chromosome stability and gene transcription⁷
76 and has been proposed to be influenced by external stimuli across a wide range of biological
77 contexts⁸⁻¹². Therefore, we hypothesised that changes to DNA methylation may be involved in
78 the bovine host response to infection with *M. bovis*; this mechanism has previously been
79 proposed for human tuberculosis caused by infection with *Mycobacterium tuberculosis*¹³.

80 Host epigenomic plasticity to *M. tuberculosis* has been reported previously^{14,15}. Sharma
81 and colleagues showed that non-CpG loci in the host genome were hypermethylated following
82 reduced representation bisulfite sequencing (RRBS) analysis of THP-1 macrophages (a human
83 monocytic cell line) infected with *M. tuberculosis*¹⁴. In addition, Zheng *et al.*¹⁵ demonstrated
84 that interleukin gene promoter sequences, and their receptors, were associated with
85 hypermethylation following analysis of THP-1 cells infected with clinical strains of *M.*
86 *tuberculosis*, using the human inflammatory response methyl-profiler DNA methylation PCR
87 array. Furthermore, it has been demonstrated that DNA methylation is associated with hypoxic
88 survival of *M. tuberculosis*¹⁶. Most recently, Doherty *et al.* reported that there were in excess of
89 750 differentially methylated regions between *M. bovis*-infected and healthy cattle in a study
90 using RRBS to examine CD4⁺ T lymphocytes isolated from circulating blood samples¹⁷.

91 A range of studies have highlighted the impact of infecting microorganisms on host DNA
92 methylation patterns. For example, distinct DNA methylation changes have been observed in
93 macrophages infected with the intracellular protozoan *Leishmania donovani*, the causative agent
94 of visceral leishmaniasis¹⁸. In addition, global DNA methylation changes have been detected in
95 human neutrophils infected with *Anaplasma phagocytophilum*, which causes granulocytic
96 anaplasmosis¹⁹. Finally, it has been proposed that, during chronic *Helicobacter pylori* infection
97 in humans, functional *H. pylori* DNA methyltransferases enter host epithelial cells and methylate
98 their recognition sequences in chromosomal DNA, potentially contributing to the pathogenesis of
99 gastric adenocarcinoma or lymphoma of the mucosa-associated lymphoid tissue²⁰.

100 Our group has previously revealed the impact of *M. bovis* infection on the mammalian
101 alveolar macrophage gene expression, demonstrating that the bAM transcriptome is substantially
102 reprogrammed as a consequence of both host-driven defence responses and mycobacterial-

103 induced perturbation and manipulation of cellular processes²¹⁻²⁴. However, the effect of *M. bovis*
104 on the bovine host epigenome, specifically the DNA methylome of bAM, remains unexplored.
105 Recent work has shown that intracellular microbial infection can lead to alterations of the host
106 DNA methylome; therefore, for the present study we used WGBS to test the hypothesis that
107 bAM DNA methylation patterns are altered during the earliest stage of *M. bovis* infection in
108 cattle.

109 **Materials and Methods**

110 **Ethics statement**

111 All animal procedures were performed according to the provisions of the Cruelty to
112 Animals Act of 1876 and EU Directive 2010/63/EU. Ethical approval was obtained from the
113 University College Dublin Animal Ethics Committee (protocol number AREC-13-14-Gordon).

114 **Isolation and infection of bovine alveolar macrophages**

115 Isolation and purification of bAM from cattle was performed as previously described by
116 our group^{21,23} and is summarized in Fig. 1. Briefly, total lung cells were harvested by pulmonary
117 lung lavage with Hank's Balanced Salt Solution (Invitrogen, Life Technologies) following the
118 removal of lungs from eight unrelated Holstein-Friesen male calves. Total lung cells were
119 washed and cultured for 24 h at 37 °C in R10⁺ media (RPMI 1640 medium supplemented with
120 antibiotics [Invitrogen]). After incubation, cells were prepared for infection by dissociation and
121 seeding at 5×10^5 viable cells/well, for each biological replicate. The purity of the seeded
122 macrophages was confirmed by flow cytometry using anti-CD14 antibody. bAM were infected
123 with *M.bovis* strain AF2122/97 at a multiplicity of infection (MOI) of 10 bacilli per alveolar
124 macrophage as described in detail previously^{21,23}. These previous studies used comparative
125 RNA-seq-based transcriptomics and targeted quantitative assays (RT-qPCR and multiplex
126 ELISA) of several NF-κB-inducible pro- and anti-inflammatory cytokines and chemokines,
127 including CCL-4, IL-1β, IL-6, IL-10 and IL-12, to verify that at 24 hours post-infection (hpi) *M.*
128 *bovis*-treated bAM cells were infected and had internalised bacilli^{21,23}.

129 **Isolation of DNA and library preparation**

130 DNA was extracted from *M. bovis*-infected bAM 24 hpi ($n = 8$) and from control bAM
131 ($n = 8$) at the same time point using the DNeasy kit (Qiagen) according to the manufacturer's
132 recommendations. DNA was quantified using the Qubit dsDNA HS Assay Kit (ThermoFisher
133 Scientific). Libraries were prepared for WGBS using the post-bisulfite conversion library
134 preparation method for methylation analysis (EpiGnome™ Methyl-Seq Kit, Epicentre, Illumina)
135 according to the manufacturer's instructions. Genomic DNA (50 ng) isolated from *M. bovis*-
136 infected or non-infected bAM (24 hpi) was bisulfite-modified (EZ Methylation-Direct Kit,
137 Zymo) according to the manufacturer's guidelines. DNA synthesis was performed by mixing
138 bisulfite-converted DNA with 2 μ l DNA synthesis primer, incubating at 95 °C for 5 min, cooling
139 on ice, followed by addition of 4 μ l EpiGnome DNA Synthesis Premix 0.5 μ l, 100 mM DTT and
140 0.5 μ l EpiGnome Polymerase. Reactions were incubated at 25 °C for 5 min followed by 42 °C
141 for 30 min, then cooled to 37 °C for 2 min before addition of 1 μ l Exonuclease I to each reaction.
142 Following this, reaction mixtures were incubated at 37 °C for 10 min, 95 °C for 3 min and then
143 held at 25 °C. DNA was di-tagged by adding 7.5 μ l EpiGnome TT Premix and 0.5 μ l DNA
144 polymerase to each reaction and incubating at 25 °C for 30 min, 95 °C for 3 min and cooling to
145 4 °C. Tagged DNA was purified using the using the AMPure XP (1.6 \times beads, 40 μ l) system. A
146 PCR step was performed to generate the second strand of DNA, complete the addition of the
147 Illumina adaptor sequences and incorporate an index sequence. 22.5 μ l of di-tagged DNA was
148 mixed with 25 μ l FailSafe PCR PreMix E, 1 μ l EpiGnome Forward PCR Primer, 1 μ l EpiGnome
149 Index PCR Primer and 0.5 μ l FailSafe PCR Enzyme (1.25 U) and subjected to an initial
150 denaturation of ds DNA at 95 °C for 1 min followed by 10 cycles of 95 °C for 30 sec, 55 °C for
151 30 sec and 68 °C for 3 min. Following PCR, the reactions were incubated at 68 °C for 7 min.

152 EpiGnome libraries were purified using the AMPure (1× beads, 50 µl) system to remove primer
153 dimers. Libraries were quantified by Qubit using the Qubit dsDNA HS Assay Kit (ThermoFisher
154 Scientific) and library quality was assessed on an Agilent BioAnalyzer using the High sensitivity
155 DNA assay kit (Agilent Technologies).

156 **Pyrosequencing**

157 Genomic DNA was extracted from *M. bovis*-infected and control bAM (isolated from a
158 parallel set of four animals to those used for WGBS) and quantified with the High-Sensitivity
159 DNA Assay Kit (Agilent Technologies). DNA (200 ng) was bisulfite-modified using the EZ
160 Methylation-Direct Kit (Zymo) and eluted in 50 µl elution buffer. Bisulfite PCR reactions were
161 performed in 25 µl consisting of 0.2 µM each primer, 2 mM MgCl₂, 1× PCR buffer (minus
162 magnesium), 0.2 mM dNTPs, Platinum *Taq* DNA polymerase (Invitrogen), and 3 µl bisulfite-
163 modified DNA. Primer sequences are detailed in Table 1. PCR cycling conditions were as
164 follows: 95 °C for 5 min followed by 40 cycles of 30 sec each at 95 °C; either 55 °C (*TNF*,
165 *NFKB2* and *IL12A*) 56 °C (*DTX4*, *CIQB* and *NOS2*) or 58 °C (*TLR2*) for 30 sec; 72 °C for
166 30 sec, and a final elongation step of 5 min at 72 °C. PCR products were verified by
167 electrophoresis on a 2% w/v agarose gel before pyrosequencing (Pyromark Q24, Qiagen).
168 Pyrosequencing assays were designed in-house and carried out as previously described^{25,26}.
169 Only pyrosequencing reactions that passed Pyromark Q24 internal controls for bisulfite
170 modification were included in the analysis. Two-tailed paired sample *t*-tests were used to assess
171 statistically significant DNA methylation between control and *M. bovis*-infected samples.

172

173

174 **Bisulfite PCR, cloning, sequencing and combined bisulfite restriction analysis**

175 Bisulfite-converted DNA from control and infected bAM was amplified in 25 μ l
176 reactions containing 0.2 μ M primers, 1 \times buffer, 0.2 mM dNTPs, 2.5 U Platinum *Taq* DNA
177 polymerase and 3 mM MgCl₂. Primer sequences are detailed in Table 1. PCR cycling conditions
178 were as follows: 95 °C for 3 min followed by 35 cycles of 30 sec each at 95 °C; 58 °C, 72 °C for
179 30 sec, and a final elongation step of 5 min at 72 °C. PCR products were purified using the
180 Wizard clean up kit (Promega) and cloned into the pJET1.2/blunt vector (Fermentas). Insertion
181 of PCR products was verified by digestion with *Bg*/III and positive clones were sequenced using
182 conventional Sanger sequencing (Eurofins Genomics). Combined bisulfite restriction analysis
183 (COBRA) was carried out using *Taq*AI, and/or *Aci*I as outlined in ²⁷. Sequence analysis and
184 alignment was performed using DNASTar EditSeq, MegAlign (www.dnastar.com) and BiQ Meth
185 Analyzer (<http://biq-analyzer.bioinf.mpi-inf.mpg.de>). During this analysis, sequences with low
186 C-T conversion rate (< 95%) and with a high number of sequencing errors (sequence identity
187 with genomic sequence less than 80%) were excluded from the alignment. Identical clones were
188 also excluded from the analysis.

189 **Illumina sequencing and initial quality control**

190 Pooled libraries were sequenced at the Michigan State University Research Technology
191 Support Facility. Paired-end reads (2 \times 150 bp) were obtained by Illumina sequencing of each
192 pooled library on four lanes of a HiSeq 2500 sequencer, in rapid run mode. After pooling data
193 from all lanes, bisulfite-treated (BS) libraries yielded 45.3–67.4 million read pairs per sample;
194 comparably, non-bisulfite (NON-BS) libraries yielded a total of 40–50 million read pairs per
195 sample across all lanes (Supplementary Table 1).

196 Quality control of raw read pairs using *FastQC*
197 (www.bioinformatics.babraham.ac.uk/projects/fastqc) revealed similar QC metrics for both
198 infected and control samples (Supplementary Table 2). Although samples from animals 1, 4, 5,
199 and 6 raised warnings of *Over-Represented Sequences*, this warning was systematically triggered
200 by N-polymers in the second mate, a technical issue resolved by quality trimming. As expected,
201 BS libraries raised significantly more *Per Base Sequence Content* and *Per Base GC Content* than
202 NON-BS libraries, due to the nature of the bisulfite treatment (Supplementary Table 2).

203 **Adapter and quality trimming**

204 Stringent adapter trimming (overlap ≥ 1 bp at the 3' end of each read), and quality
205 trimming (Phred ≤ 20 from the 3' end of each read) using *Trim Galore!* [version 0.4.1]
206 (www.bioinformatics.babraham.ac.uk/projects/trim_galore) left 97.5–98.4% of raw read pairs in
207 bisulfite-treated samples, and 93.1–94.3% of raw read pairs for NON-BS samples. However, this
208 trend was reversed at the nucleotide level, with 77.5–86.9% of sequenced bases left in BS
209 libraries, against 84.8–87.3% in NON-BS libraries. Notably, BS libraries generally showed
210 higher levels of adapter contamination (54.2–77.3% of raw reads) relative to NON-BS libraries
211 (48.6–58.2% of raw reads), based on the stringent detection rule described above. Second read
212 mates displayed a larger proportion of low-quality sequenced bases trimmed (7.6–13.5% of raw
213 sequenced bases) relative to first mates (1.9–4.5% of raw sequenced bases), in both BS and
214 NON-BS libraries (Supplementary Table 1).

215 Notably, quality control of trimmed libraries revealed a significant improvement of *Over-*
216 *Represented Sequences*, and full resolution of *Adapter Content* warnings (data not shown). As a
217 result of stringent adapter trimming (even a single trailing A at the 3' end was trimmed;
218 following Trim Galore! default settings), all samples raised warnings of *Per Base Sequence*

219 *Content* caused by the severe under-representation of A nucleotides at the 3' end of reads, a
220 known artefact of the stringent trimming process with no notable repercussion on the subsequent
221 alignments and methylation calls.

222 **Alignment of bisulfite-treated libraries**

223 BS libraries were aligned using *Bismark* [version 0.15.2]²⁸ and the *Bowtie2* aligner
224 [version 2.2.6]²⁹ in strand-specific (directional) mode to computationally generate bisulfite-
225 converted copies of the top and bottom strands of the *Bos taurus* UMD3.1 genome assembly³⁰.
226 Alignment efficiency (*i.e.*, read pairs aligned to a unique locus) reached 59.7–68.3%, for a total
227 of 28.8–42.7 million read pairs aligned uniquely per sample. Aligned reads were found evenly
228 distributed between the top and bottom strands of the BS-converted genome (Supplementary
229 Table 3). Bismark methylation calls revealed methylation levels in the range of 69.2–73.8% in
230 CpG context, for a total of 113–156 million methylation calls per sample. In contrast, non-CpG
231 context displayed markedly low methylation levels (0.7–1.7%), with orders of magnitude larger
232 counts of methylation calls, owing to their broader definition of methylation context (392–543
233 million calls in CHG context; 1.1–1.5 billion calls in CHH context: H corresponds to A, T or C).

234 **Deduplication of aligned bisulfite-treated libraries**

235 Paired-end alignments where both mates aligned to the same position in the genome were
236 removed from the Bismark alignment output using the *deduplicate_bismark* script to mitigate the
237 impact of duplicate DNA fragments sequenced. This procedure discarded 6.1–18.8% aligned
238 read pairs, leaving 25.5–38.7 million aligned read pairs for subsequent methylation calls
239 (Supplementary Table 4).

240

241 **Methylation calls**

242 The *bismark_methylation_extractor* script was used in a two-pronged approach. First,
243 methylation calls extracted from the full sequence of aligned read pairs were used to evaluate *M*-
244 bias across the aligned mates. *M*-bias plots show the methylation proportion across each possible
245 position in the read, and reveal anomalies at any position of the sequenced reads, often found
246 toward ends of the sequenced reads. After analysis of the *M*-bias plots generated in the first pass,
247 the second call to the *bismark_methylation_extractor* script was set to ignore the first seven
248 bases at the 5' end of both read mates. Collated reports of the Bismark pipeline leading to the
249 final methylation calls are available as HTML files in Supplementary File 1.

250 **Statistical analyses**

251 Methylation calls in CpG context were imported from the individual Bismark CpG
252 reports, combined and processed in a *BSseq* container of the *bsseq* Bioconductor package
253 [version 1.9.2; www.bioconductor.org/packages/bsseq] ³¹. Genomic coordinates of CpG islands
254 on all sequences (*i.e.*, unmasked sequence CpG island track) in the UMD3.1/bosTau6 assembly
255 were obtained from the UCSC Table Browser ³².

256 **Non CpG methylation**

257 Non-CpG methylation (CHH and CHG) present in the WGBS reads were analysed using
258 the methylKit R package ³³. De-duplicated bam files produced during alignment with Bismark
259 were sorted and saved as sam formatted files. Individual CHH or CHG were imported separately.
260 These files were imported to the methylKit object using strict criteria: at least 10× coverage per
261 feature and the feature must be present across all samples. This resulted in a total of 685,311 and
262 284,641 features for CHH and CHG respectively, with a median coverage of 40× for CHH and

263 41× for CHG. Median coverage between all samples was used to calculate a scaling factor to
264 normalize the coverage across samples. Differential methylation was determined for individual
265 features with an overdispersion parameter included (shrinkMN) and Benjamini-Hochberg (B-H)
266 FDR adjustment for multiple comparisons³⁴. All downstream analyses were carried out
267 separately for CHH and CHG methylation. Average methylation between groups was tested
268 using a paired *t*-test.

269 **Expression dynamics of genes associated with chromatin configuration and DNA** 270 **methylation**

271 For the bAM samples used for the WGBS analysis at 24 hpi described here, differentially
272 expressed genes were previously identified in the same *M. bovis*-infected bAM, relative to the
273 non-infected bAM at 2, 6, 24 and 48 hpi using RNA-seq²³. A comprehensive list (EPI-list) of
274 151 genes previously identified as being involved with histone modifications or DNA
275 methylation was generated from the literature (Supplementary File 2). RNA-seq transcriptomics
276 data was mined, at each time point, using the EPI-list. Ultimately, 86 genes were identified from
277 the RNA-seq data (Supplementary File 2). These 86 genes were denoted as genes of interest
278 (GOI) and their expression was determined at 2, 6, 24 and 48 hpi using the previously published
279 lists of differentially expressed genes ($P < 0.05$, B-H FDR-adjusted).

280 **Gene ontology enrichment analyses**

281 Gene ontology enrichment analyses were performed using the Bioconductor *GOseq*
282 software package³⁵ and the annotation package *org.Bt.eg.db*
283 (<https://bioconductor.org/packages/org.Bt.eg.db>). Notably, the probability weighting function
284 (PWF) supplied to *GOseq* was calculated without length bias for the analysis of promoters, as

285 those were defined in this study to a constant width of 2 kb (1.5 kb upstream and 500 bp
286 downstream of TSS).

287 **Results**

288 **WGBS summary statistics**

289 In summary, 16 individually barcoded WGBS libraries, prepared using bAM DNA
290 extracted from eight *M. bovis*-infected and eight non-infected samples, were sequenced on an
291 Illumina HiSeq 2500 sequencer in rapid run mode. This generated 45.3–67.4 million read pairs
292 per sample and ~32× sequencing depth per condition (*M. bovis*-infected and non-infected bAM).
293 These data satisfy previously defined criteria for WGBS, with respect to the number of
294 independent biological replicates and the sequencing depth
295 (www.roadmappigenomics.org/protocols)³⁶. An assessment of bisulfite conversion rates was
296 performed using non-CpG methylation according to Clark *et al.*³⁷. Based on this approach,
297 conversion efficiencies were > 99% using CHH methylation values and > 98% using CHG
298 methylation values.

299 When all CpG dimers in the reference bovine genome (UMD3.1) were considered—
300 approximately 55.1 million stranded loci, including potentially unmappable CpG dimers—the
301 25.5–38.7 million aligned read pairs used for methylation calls led to an average 1.1–1.4
302 methylation call per individual strand-specific CpG dimer in each individual sample. As a result
303 of collapsing methylation calls as unstranded CpG loci, the even distribution of aligned read
304 pairs on both strands of the reference genome (Supplementary Table 3) doubled coverage to
305 2.12–2.78× per unstranded CpG dimer (~27.5 million unstranded loci). Unstranded methylation
306 calls were used from this point onwards. While the mean coverage of CpG dimers covered in at
307 least one sample was similar (2.13–2.81×; ~27.3 million loci), CpG dimers covered in all
308 samples was larger for each sample (4.6–5.9×; 4.7 million loci). Notably, the average coverage

309 of all CpG dimers in known CpG islands (CGIs)—including CpG dimers with null coverage—
310 was similar to those latter values (3.9–5.4×; 2.9 million loci), suggesting a consistent coverage of
311 CGIs across all samples.

312 **Genome-wide scan for differentially methylated regions 24 hpi**

313 An unbiased genome-wide scan was performed to identify potential differentially
314 methylated regions (DMRs), including only CpG loci with at least two methylation calls for at
315 least six of the eight biological replicates in each sample group, thereby ensuring at least 12×
316 coverage for any CpG dimer in both sample groups. As a comparison, the analysis was repeated
317 after randomising samples from both infection groups to produce a distribution of *t*-statistics
318 under the null hypothesis. The *bsseq* package was used to calculate *t*-statistics in a paired design
319 for both original and randomised sets of sample (Fig. 2A and 2B).

320 Potential DMRs were identified as genomic regions including at least three loci with
321 absolute *t*-statistics greater than 4.6 and a mean difference in methylation level (across samples
322 and loci) greater than 10% between the two groups. This analysis did not reveal significant
323 differences in methylation between infected and non-infected bAM; regions identified in the
324 original data were comparable to randomised data in number of regions identified and their
325 properties (*e.g.*, width, number of methylation loci, sum of *t*-statistics, proportion of regions
326 showing increased and decreased methylation level) (Supplementary Table 5).

327 **Distribution of methylation across different genomic regions**

328 Following the genome-wide scan, DNA methylation was determined at the following
329 defined functional genomic elements: gene bodies, intergenic sequences and proximal promoters.
330 Genomic elements were defined as described previously by Peat and colleagues³⁸ and the

331 number of regions compared in each category are outlined in Table 2. As expected for a
332 differentiated/somatic cell type, the majority of CpGs within intragenic sequences, gene bodies
333 and CpG-deficient promoters were widely methylated^{39,40}. CpG-rich promoters containing a
334 CpG island (CGI) or overlapping a CGI (Promoter CGI and CGI promoter) were mostly
335 hypomethylated (Fig. 3). Interestingly, CGIs remote from annotated gene promoters (non-
336 promoter CGIs) showed variable methylation—most were hypermethylated (>75% methylated,
337 18,581 CGIs) with 9,103 non-promoter CGIs hypomethylated (<25%).

338 **Pyrosequencing validation of WGBS at key immune function genes**

339 To confirm the WGBS observation that DNA methylation was not different between
340 control and infected bAM, 24 hpi, a small panel of key immune genes, *TNF*, *IL12A*, *TLR2*,
341 *NFKB2*, *CIQB*, *NOS2* and *DTX4* were selected for targeted analysis by pyrosequencing.
342 Transcription of these genes has previously been shown to be upregulated in bAM 24 hpi with
343 *M. bovis*^{21,23}; the specific loci that were analysed by pyrosequencing are detailed in Fig. 4. Four
344 of the loci are hypomethylated (*TNF*, *IL12A*, *TLR2* and *NFKB2*), one is intermediately
345 methylated (*NOS2*) and two are highly methylated (*CIQB*). Using DNA isolated from a parallel
346 set of control ($n = 4$) and infected ($n = 4$) bAM samples, average methylation levels at the
347 proximal promoter regions of *NFKB2*, *TLR2*, *IL12A* and *TNF*, and the gene bodies of *CIQB*,
348 *NOS2* and *DTX4*, were determined. Statistical analysis using a paired *t*-test did not reveal
349 significant differences ($P \geq 0.05$) in mean methylation levels between the examined loci of
350 infected and non-infected bAM samples (Fig. 5), supporting the WGBS observation that *M.*
351 *bovis* does not have an effect on the CpG methylation in bAM.

352

353 **Promoter methylation level and gene ontology in bovine alveolar macrophages**

354 Leveraging the absence of significant DMRs between infected and non-infected bAM
355 samples, methylation calls were pooled across all sixteen samples (eight *M. bovis*-infected and
356 eight controls) to analyse methylation levels in bAM gene promoters, with maximal coverage. In
357 this analysis, promoters were defined as regions spanning 1.5 kb upstream and 500 bp
358 downstream of each transcription start site (TSS), with a minimum of 10 CpGs each associated
359 with at least five methylation calls were included (26.8 million loci). Of the 24,616 genes
360 annotated in the bovine genome (Ensembl BioMart March 2016 archive), 22,964 were retained
361 for this analysis, on the basis that their promoter contained at least ten loci, each locus having at
362 least five methylation calls. For those genes, mean promoter methylation was estimated and
363 summarised, alongside average gene body methylation, in Fig. 2C.

364 Notably, the vast majority of gene promoters were found at either extreme of the
365 methylation range. Indeed, 18,438 promoters (80.3%) display methylation levels greater than
366 75% or lower than 25% (8,145 \geq 75% methylated; 10,293 \leq 25% methylated). However, 2,580
367 promoters (9.7%) displayed an average intermediate methylation level (IM, 33–66%). Strikingly,
368 gene ontology (GO) analysis of the genes associated with IM promoters (33–66%) using the
369 *GOseq* package³⁵ revealed a marked enrichment for immune-related GO categories including
370 “defense response” ($P < 10^{-08}$), “defense response to bacterium” ($P < 10^{-07}$), “response to
371 bacterium” ($P < 10^{-07}$), “chemokine-mediated signaling pathway” ($P < 10^{-06}$) and “chemokine
372 activity” ($P < 10^{-04}$), among others (Supplementary Table 6). In contrast, no significant
373 enrichment for immune-related GO categories was found for promoters with methylation levels
374 0–1% (759 promoters), 0–10% (5,605), 10–20% (3,255), or 90–99% (1,997) (Supplementary

375 Table 6). Instead, the latter only suggested enrichment for generic GO categories (*e.g.*,
376 “intracellular organelle”, “transcription regulatory region DNA binding”).

377 A hallmark of some imprinted genes is that they contain a 5' differentially methylated
378 region that is IM (resulting from parent-of-origin specific methylation patterns); therefore, the
379 IM promoter list was interrogated for known bovine imprinted genes
380 (www.geneimprint.com/site/genes-by-species.Bos+taurus). This analysis confirmed IM at the
381 promoters of the following imprinted genes; *PLAGL1*, *SNRPN*, *MEST*, *PEG10*, *GNAS* and *NNAT*
382 (Supplementary Fig. 1).

383 **Targeted analysis of intermediately methylated (IM) gene promoters**

384 To confirm the presence of IM at immune gene promoters, COBRA and clonal analysis
385 of bisulfite PCR products was performed. Firstly, proximal promoter alignment plots for the IM
386 group were visually screened to remove promoters that were included due to averaging of
387 sequences with high and low methylation (example of this in Fig. 6). This analysis was restricted
388 to IM promoters containing a minimum of 30 CpGs (1,034 loci), to ensure sufficient CpG
389 coverage during COBRA and clonal bisulfite sequencing analysis. Of the 1,034 IM promoters,
390 267 promoters remained in the IM group and 60/267 (22.5%) of them had a promoter CGI
391 (Supplementary File 3). GO analysis of these 267 IM gene promoters with ≥ 30 CpGs revealed
392 enrichment for NADH dehydrogenase-associated activity (Supplementary Table 6). Two
393 immune-related gene promoters with the highest CpG content, *CIQB* and *IL2RA*, were selected
394 for further analysis (Fig. 7). Clonal analysis revealed that, although there are clearly
395 hypermethylated and hypomethylated *CIQB* and *IL2RA* alleles, the prominent allelic
396 methylation pattern is mosaic (Figs. 8 and 9); suggesting that the IM promoters analysed are

397 methylated in an allele-independent as opposed to an allele-specific pattern, an observation that
398 has been previously reported⁴¹. To further confirm our WGBS and clonal bisulfite sequencing
399 results we carried out COBRA on *CIQB* and *IL2RA* IM regions, using *M. bovis*-infected and
400 non-infected bAM (Fig. 8 and 9). Results from COBRA support our observation that the *CIQB*
401 and *IL2RA* proximal promoters were IM. Additionally, bovine sperm, kidney, liver and heart
402 samples were assessed using COBRA to determine whether IM might be tissue-specific.
403 COBRA indicated that *IL2RA* was almost completely methylated in sperm and predominantly
404 methylated in the kidney, liver and heart; suggesting a potential tissue-specific IM in bAM (Fig.
405 9). This possible tissue-specific IM pattern was not observed at the *CIQB* locus (Fig. 8).

406 **Non-CpG methylation analysis**

407 Overall, we found a low level of methylation in the context of CHH: mean values of
408 0.98% and 0.96% were estimated for control and *M. bovis*-infected bAM, respectively (Fig. 10).
409 CHH methylation was not different between control and infected-bAM (t -statistic 1.32,
410 $df = 12.7$, $P > 0.05$). Similarly, for CHG methylation we found an overall low mean methylation
411 of 1.53% and 1.49% for control and *M. bovis*-infected bAM, respectively (Fig. 10). There was no
412 difference for this mean methylation in CHH context between groups (t -statistic 1.26, $df = 13.5$,
413 $P > 0.05$). Neither clustering on all data nor top 5,000 most variable features revealed any
414 patterns in these data sets for CHH and CHG methylation. This was also concordant with
415 differential methylation tests showing no loci as significantly differentially methylated between
416 groups by a methylation difference greater than 1% and q -value = 0.01.

417

418

419 **Relationship between *M. bovis* infection and expression of chromatin and DNA modifiers**

420 Based on our WGBS results, bAM DNA methylation is not affected by infection with
421 *M. bovis* at 24 hpi; therefore, we next determined whether *M. bovis* infection has an effect on
422 chromatin. To do this, transcription analysis of chromatin and DNA modifying enzymes was
423 carried out using our previously published RNA-seq data from *M. bovis*-infected bAM²³ and a
424 similar approach to that detailed by Nestorov and colleagues⁴². A list of 151 genes (EPI-list) that
425 encode chromatin and DNA modifying enzymes was assembled from the literature
426 (Supplementary File 2). To identify chromatin and DNA modifying-associated genes that were
427 detected by RNA-seq, differentially expressed genes ($P < 0.05$, B-H FDR-adjusted) at each time
428 point were compiled and searched using the list of 151 known genes. This identified a list of 86
429 genes of interest (GOI). The number of GOIs was determined at each time point and the results
430 were as follows: 2 hpi 0/86, 6 hpi 8/86 (3 upregulated, 5 downregulated), 24 hpi 37/86 (16
431 upregulated, 21 downregulated) and 48 hpi 48/86 (19 upregulated, 29 downregulated)
432 (Supplementary File 2). *HDAC5*, *KDM2B*, *EZH1*, *PRDM2*, *SETMAR*, *SMYD4* and *USP12* were
433 differentially expressed at all time points post-infection (excluding 2 hpi).

434 Discussion

435 Here we present genome-wide DNA methylation profiles of bAM infected with *M. bovis*
436 versus non-infected controls at 24 hpi. We show that CpG methylation in bAM is not altered in
437 response to *M. bovis* at 24 hpi. Since previous studies suggest that DNA methylation changes are
438 established relatively late in the silencing pathway and are preceded by alterations to histone
439 modifications and chromatin packing⁴³, our results may reflect the early post-infection time
440 point examined in this study. Examination of the WGBS data, focusing on the relationship
441 between DNA methylation and proximal promoters, revealed an enrichment of gene promoters
442 that were intermediately methylated.

443 Global methylation patterns were first analysed using an unbiased genome-wide scan to
444 identify differentially methylated loci between *M. bovis*-infected and control bAM. Following
445 this, we examined the impact of infection on the bAM methylome in greater detail by assessing
446 DNA methylation at specific genomic features. Given the relationship between promoter
447 methylation, gene body methylation and transcription⁴⁴, these genomic features comprised the
448 main focus of these analyses. Promoters and CGIs were separated into the following categories
449 as previously described³⁸: CGI promoters (*i.e.*, gene promoters overlapping a CpG island), non-
450 CGI promoters, promoter CGIs and non-promoter CGIs. None of these approaches revealed any
451 differentially methylated loci between *M. bovis*-infected and non-infected control bAM at 24 hpi.
452 Therefore, it is unlikely that the substantial transcriptomic perturbation observed in bAM during
453 the first 24 h of *M. bovis* infection²³ is due to reconfiguration of CpG methylation patterns. On
454 the other hand, the results presented here indicate that cell signalling and transcription factor-
455 driven gene regulatory transduction cascades lead to the rapid transcriptional activation of
456 immune- and other genes. This observation is supported by previous work showing that DNA

457 methylation changes in THP-1 macrophages infected with *M. tuberculosis* do not occur at CpGs
458 ¹⁴. In their study, Sharma and colleagues demonstrated that methylation was perturbed at non-
459 CpGs. Similarly, Lyu *et al.* recently demonstrated that infection of human THP-1 macrophages
460 with virulent and avirulent *M. tuberculosis* is not associated with host DNA methylation changes
461 ⁴⁵. Unlike THP-1 macrophages infected with *M. tuberculosis*, we show that non-CpG
462 methylation is not altered in bAM infected with *M. bovis*. The lack of differences in non-CpG
463 methylation may be explained, in part, by the differences in cell types used—comparing a
464 macrophage-like human cell line (THP-1) to a primary, differentiated bovine macrophage.
465 Mycobacteria have recently been reported to modulate the host immune response through
466 chromatin modifications ^{46,47}. Given the absence of differential CpG methylation between non-
467 infected and *M. bovis*-infected bAM at 24 hpi, and the differential expression of genes encoding
468 chromatin modifiers observed in the current study, it is reasonable to hypothesise that chromatin
469 reconfiguration may have a role in regulating host gene expression in response to infection with
470 *M. bovis*.

471 To comprehensively annotate gene promoter methylation in bAM we quantified average
472 DNA methylation at proximal promoter regions spanning the TSS (1,500 bp upstream and
473 500 bp downstream). As expected, the majority of promoters containing or overlapping a CGI
474 were hypomethylated and those promoters not associated with CGIs were, generally, highly
475 methylated ⁴⁸. However, a large number of promoters (2,580) exhibited mean methylation levels
476 ranging between 33–66% (intermediately methylated; IM). Interestingly, in addition to this, gene
477 ontology analysis of the genes proximal to these promoters indicated a marked enrichment for
478 immune-function related categories. Further analysis of the IM promoter group revealed that
479 most promoters were included due to averaging of methylated and unmethylated CpGs within

480 the 2 kb promoter regions. After removing these promoters, 267 promoters remained that
481 exhibited IM. Validation experiments, using clonal analysis and COBRA, confirmed
482 intermediate DNA methylation at the proximal promoter of two of these non-imprinted IM
483 genes, *CIQB* and *IL2RA*. Six of the 267 promoters were proximal to known bovine imprinted
484 genes, displaying predominant intermediate methylation of 5' CGIs; as expected for imprinted
485 genes in an adult somatic cell type ⁴⁹. The remaining promoters are IM non-imprinted genes.
486 Previous work by Weber and co-workers demonstrated that, in somatic cells, the concentration
487 of CpGs within a gene promoter is related to the level of DNA methylation; promoters with a
488 high frequency of CpGs (HCP) tend to be unmethylated and promoters with a lower CpG content
489 (LCP) tend to be methylated ⁴⁸. Sixty of the 267 IM promoters identified in this study contained
490 high frequencies of CpGs (CGIs) normally associated with unmethylated HCPs, suggesting that
491 promoter IM in bAM is occurring irrespective of CpG density. It has been suggested that
492 intermediate DNA methylation is a conserved signature of genome regulation associated with
493 intermediately active rather than suppressed gene expression ⁴¹. It is possible that these
494 intermediately methylated promoters are a hallmark of bAM and functionally associated with
495 this particular cell type. However, Elliot and colleagues demonstrated that different tissues and
496 cell types are intermediately methylated equally ⁴¹; therefore, the function of intermediate
497 methylation at these genomic loci remains to be fully elucidated.

498 **Conclusion**

499 This is the first comprehensive analysis of the mammalian alveolar macrophage DNA
500 methylome in response to infection with a mycobacterial pathogen. Although the epigenome of
501 host bAM was not perturbed by a 24 h exposure to the pathogenic bacterium, *M. bovis*, this work
502 provides the first annotation of genome-wide DNA methylation patterns in the bovine genome

503 and is directly aligned with the goal of the Functional Annotation of Animal Genomes (FAANG)
504 project to ‘*produce comprehensive maps of functional elements in the genomes of domesticated*
505 *animal species*’⁵⁰. Furthermore, this work also provides evidence for differential methylation at
506 the proximal promoter regions of more than 200 non-imprinted genes.

507

508

509 **Acknowledgments**

510 We would like to thank Felix Krueger of the Babraham Institute for advice on WGBS data
511 processing and quality control and for providing permission to use the Bismark Reports and
512 Babraham Bioinformatics logos, located in the supplementary information. In addition, we
513 would like to thank Han Haige for assistance with translation of a Chinese journal article.

514 **Author Contributions** Conceived and designed the experiments: AMOD, DAM, SVG and
515 DEM. Prepared the samples: DAM and JB. Performed the experiments: AMOD, DAM, SA and
516 REI. Provided RNA-seq data: NCN. Analysed the data: KRA, MWW, AMOD, SA and TJH.
517 Prepared the manuscript: AMOD, KRA and DEM. All authors read and approved the
518 manuscript.

519 **Disclosure of interest** The authors report no conflict of interest.

520 **Data availability** All WGBS data is available from NCBI GEO ⁵¹ (Accession Number
521 GSE110412).

522 **Figure Legends**

523 **Figure 1. Schematic representation of sample preparation.** Bovine alveolar macrophages
524 (bAM) were isolated, post-mortem, from the lungs of age-matched male Holstein-Friesian calves
525 by lavage. Purity of the cells was confirmed using flow cytometry with anti-CD14. Isolated cells
526 were washed and seeded for 24 h prior to infection. Infected bAM were exposed to *M. bovis* at a
527 multiplicity of infection ratio of 10:1 for 2 h. After 2 h the media was replaced in control and
528 infected samples and cells were harvested after 24 h for analysis of DNA methylation. This
529 figure was prepared by A.M.O'D. using the Biomedical PPT toolkit suite (www.motifolio.com).

530 **Figure 2. (A)** Distribution of paired *t*-statistics between *M. bovis*-infected and control non-
531 infected bAM samples based on smoothed WGBS data. **(B)** Distribution of paired *t*-statistics
532 between randomised samples based on smoothed WGBS data. **(C)** Distribution of average
533 methylation level (%) in promoters and gene bodies across all samples. Only CpG loci with
534 coverage greater or equal to 10 were considered. Only genes where gene body and promoter both
535 had 10 or more sufficiently covered CpG loci were considered.

536 **Figure 3. Distribution of DNA methylation in different genomic contexts in non-infected**
537 **and *M. bovis*-infected bovine alveolar macrophages (24 hpi).** Analysis of WGBS data from *M.*
538 *bovis*-infected and non-infected bovine alveolar macrophages (bAM) revealed that genomic
539 methylation, in the context of CpGs, was not altered at any of the sequence features outlined
540 (intergenic regions, gene bodies, or promoters with or without CpG islands (CGIs) in the host
541 following infection. Blue and red violins represent non-infected and *M. bovis*-infected bAM,
542 respectively.

543 **Figure 4. Schematic representation of WGBS data at loci related to immune function.**
544 WGBS proximal promoter plots. Representative plots showing the average methylation spanning
545 a 10 kb region at the 5' end of the *TNF*, *IL12A*, *TLR2*, *NFKB2*, *DTX4*, *CIQB* and *NOS2* genes.
546 The red and blue lines represent average methylation levels for infected and control samples,
547 respectively.

548 **Figure 5. Pyrosequencing validation of whole-genome bisulfite sequencing (WGBS) results.**
549 Locations of the pyrosequencing assays are denoted by 'PCR' in Fig. 4. Methylation was not
550 different at any of the loci tested (paired *t*-test $P \geq 0.05$) between *M. bovis*-infected and non-
551 infected control bAM. The number of CpG dinucleotides analysed at each loci were *TNF* (9

552 CpGs), *IL12A* (11 CpGs), *TLR2* (9 CpGs), *NFKB2* (8 CpGs), *CIQB* (4 CpGs), *DTX4* (3 CpGs)
553 and *NOS2* (1 CpG).

554 **Figure 6. Analysis of promoters with highly methylated and unmethylated sequence.** 1,034
555 proximal promoters, with a minimum of 30 CpGs, shown to be intermediately methylated (IM)
556 in the WGBS analysis were visually inspected to remove false positives. 767 were eliminated
557 from the IM group due to averaging of highly methylated and unmethylated CpGs in the
558 proximal promoter region (green dashed box). Four examples are presented here: the *GUCY2D*,
559 *SYN1*, *RRP1B* and *FOXRED2* genes. Red and blue lines represent average methylation levels for
560 infected and control samples, respectively.

561 **Figure 7. Gene promoters for combined bisulfite restriction analysis (COBRA) and clonal**
562 **analysis.** WGBS alignments at the *CIQB* and *IL2RA* gene loci. Each panel represents a 10 kb
563 region at the 5' end of the gene. Green dashed boxes illustrate the *CIQB* and *IL2RA* proximal
564 promoter regions (the TSS minus 1.5 kb, plus 500 bp) identified as intermediately methylated
565 (IM) during WGBS data analysis (average methylation 33–66%). PCR: region analysed using
566 bisulfite PCR, cloning and Sanger sequencing; CGIs: CpG islands; Gene: transcribed region;
567 Exons: shows the location of the first exon; Red line: *M. bovis*-infected bAM; Blue line: non-
568 infected control bAM.

569 **Figure 8. Confirmation of an intermediately methylated promoter region at the *CIQB* gene**
570 **locus. (A)** Clonal analysis of seven CpG dinucleotides in a 269 bp fragment of the bovine *CIQB*
571 5' promoter region, *a–d* represent sequencing of four biological replicates. Closed and open
572 circles denote methylated and unmethylated CpGs, respectively. **(B)** Aggregated representation
573 of methylation status at CpGs 1-7 in the *CIQB* proximal promoter region; (a)-(d) represent

574 animals A-D, numbers between boxes indicate genomic distance between CpGs while numbers
575 above boxes indicate the position of the CpG within the analysed region; BLUE = methylated,
576 BLACK = unmethylated, GREY = not present; (C) Schematic representation of the analysed
577 C1QB region and the recognition sites of *AciI* and *TaqαI* as obtained by NEBcutter V2.0; length
578 is displayed in bp; (D) – (F) COBRA results of Uninfected (D), Infected (E) and tissue samples
579 (F) digested with *AciI*, *TaqαI* or undigested (Ctrl).

580 **Figure 9. Confirmation of an intermediately methylated promoter region at the *IL2RA***
581 **gene locus.** (A) Clonal analysis of 10 CpG dinucleotides in a 378 bp fragment of the bovine
582 *IL2RA* 5' promoter region, *a–d* represent sequencing of four biological replicates. Closed and
583 open circles denote methylated and unmethylated CpGs, respectively. (B) Aggregated
584 representation of methylation status at CpGs 1-10 in the *IL2RA* proximal promoter region; *a–d*
585 represent animals A-D, numbers between boxes indicate genomic distance between CpGs while
586 numbers above boxes indicate the position of the CpG within the analysed region; BLUE =
587 methylated, BLACK = unmethylated, GREY = not present; (C) Schematic representation of the
588 analysed *IL2RA* region and the recognition sites of *TaqαI* as obtained by NEBcutter V2.0; length
589 is displayed in bp; (D) – (F) COBRA results of Uninfected (D), Infected (E) and tissue samples
590 (F) digested with *TaqαI* or undigested (Ctrl).

591 **Figure 10. Non-CpG methylation levels differ but not significantly in bovine alveolar**
592 **macrophages (bAM) infected with *Mycobacterium bovis*.** Mean methylation at the non-CpG
593 contexts CHG (left) and CHH (right) for control and *M. bovis*-infected bAMs, respectively:
594 differences were not significant by *t*-statistic.

595

596 **Table 1** Primers use for targeted DNA methylation analysis.

Gene Name	Ensembl ID	Forward primer 5'-3'	Reverse Primer 5'-3'	Sequencing Primer 5'-3'
Tumour necrosis factor alpha	TNF ENSBTAG00000025471	AGTAATTGGTTTAGAGA AGTTTATTTAGAA	CTTCCTTAATAAAAAAACC CATAAACTCAT BIOTIN*	GGTTTAGAGAAGTTTAT TTAGAAT
Interleukin 12A	IL12A ENSBTAG00000015150	TAATTAGAGAGTTAGGTT G GTTATTTATTG BIOTIN*	ATAAAAATATAACCCCT AATTTAACCTCC	CAACCACCACCCTCA
Toll-like receptor 2	TLR2 ENSBTAG00000008008	GGGGATGTTAGAGGATTT TAATTTTTGAT BIOTIN*	ACCCCAACCCCTC CTCC	CTAAACCACAAAATTAC
Complement C1q B Chain (pyroseq)	C1QB ENSBTAG00000011196	GGGGGTTTTGGGTAA TGG	AACTAAACTAATCTCC TTTAAACTCAC	GGAGATATTAGAGTAAA GGTT
Nitric oxide synthase 2	NOS2 ENSBTAG00000006894	GGGGTTTGGTGTAG TTATTGT	CTACCTAATTCTAACCAC TAACCTCTACT BIOTIN*	TGTGAAGGAGGAAGG
Deltex E3 ubiquitin ligase 4	DTX4 ENSBTAG00000004046	GAAGTTTTAGAGTTAG GGTGGATATTAGTT	TCCCAATCCTCAACATCC TCTCAT BIOTIN*	GTTAGGGTGGATATTA GTTT
Nuclear Factor Kappa-B, Subunit 2	NFKB2 ENSBTAG00000006017	TTTGGTGGTGGGAG AGGT BIOTIN*	CCTCCTCCCACCCTT ACC	ACCACCCAAAATCTAA
Complement C1q B Chain	C1QB ENSBTAG00000011196	AGAATTTGAATTAGGGTT TTTGAT T	AAACACTTTCAAATCCC ATTTCTA	n/a
Interleukin 2 receptor subunit alpha	IL2RA ENSBTAG00000020892	TTAGGGTATTATGGTGAG AGAATTAAG	AAAAAAACAAAAAATT CCCACTAC	n/a

* Denotes which primer in the pyrosequencing assay that was HPLC purified and 5' Biotinylated

597

Table 2 Number of tiles/regions in each category.

Region	Control	<i>M. bovis</i>
Intergenic	347,561	347,561
Gene Body	166,466	166,466
CGI Promoters	12,047	12,047
Non-CGI Promoters	13,413	13,413
Promoter CGIs	11,222	11,222
Non-Promoter CGIs	30,284	30,284

References

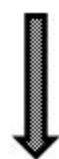
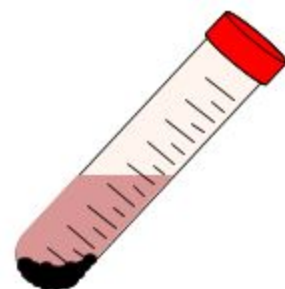
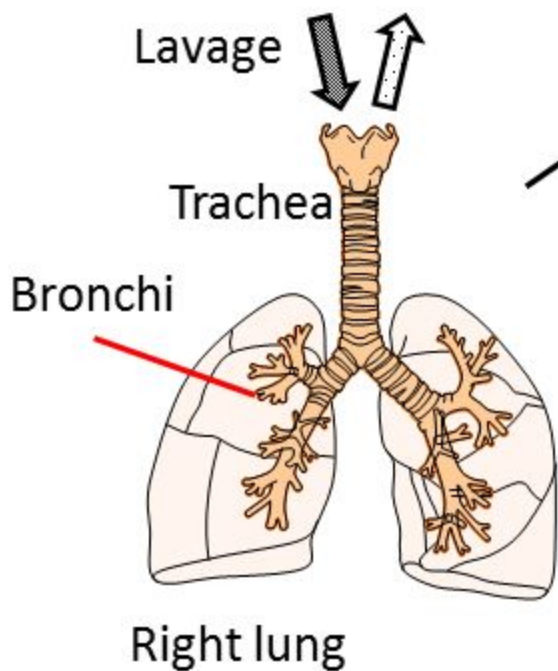
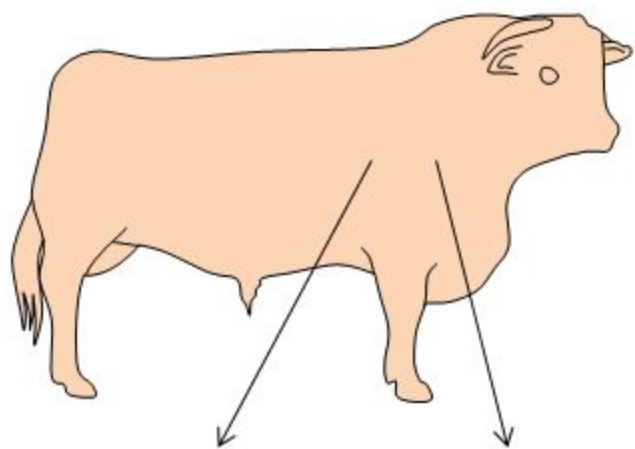
- 1 Garnier, T. *et al.* The complete genome sequence of *Mycobacterium bovis*. *Proc. Natl. Acad. Sci. U. S. A.* **100**, 7877-7882, doi:10.1073/pnas.1130426100 (2003).
- 2 Olea-Popelka, F. *et al.* Zoonotic tuberculosis in human beings caused by *Mycobacterium bovis*-a call for action. *Lancet Infect. Dis.* **17**, e21-e25, doi:10.1016/S1473-3099(16)30139-6 (2017).
- 3 Kathirvel, M. & Mahadevan, S. The role of epigenetics in tuberculosis infection. *Epigenomics* **8**, 537-549, doi:10.2217/epi.16.1 (2016).
- 4 Holoch, D. & Moazed, D. RNA-mediated epigenetic regulation of gene expression. *Nat. Rev. Genet.* **16**, 71-84, doi:10.1038/nrg3863 (2015).
- 5 Jaenisch, R. & Bird, A. Epigenetic regulation of gene expression: how the genome integrates intrinsic and environmental signals. *Nat. Genet.* **33 Suppl**, 245-254, doi:10.1038/ng1089 (2003).
- 6 O'Doherty, A. M. & McGettigan, P. A. Epigenetic processes in the male germline. *Reprod. Fertil. Dev.* **27**, 725-738, doi:10.1071/rd14167 (2015).
- 7 Yong, W. S., Hsu, F. M. & Chen, P. Y. Profiling genome-wide DNA methylation. *Epigenetics Chromatin* **9**, 26, doi:10.1186/s13072-016-0075-3 (2016).
- 8 Gonzalez, R. M., Ricardi, M. M. & Iusem, N. D. Epigenetic marks in an adaptive water stress-responsive gene in tomato roots under normal and drought conditions. *Epigenetics* **8**, 864-872, doi:10.4161/epi.25524 (2013).
- 9 Kucharski, R., Maleszka, J., Foret, S. & Maleszka, R. Nutritional control of reproductive status in honeybees via DNA methylation. *Science* **319**, 1827-1830, doi:10.1126/science.1153069 (2008).
- 10 Navarro-Martin, L. *et al.* DNA methylation of the gonadal aromatase (*cyp19a*) promoter is involved in temperature-dependent sex ratio shifts in the European sea bass. *PLoS Genet.* **7**, e1002447, doi:10.1371/journal.pgen.1002447 (2011).
- 11 O'Doherty, A. M. *et al.* Negative energy balance affects imprint stability in oocytes recovered from postpartum dairy cows. *Genomics* **104**, 177-185, doi:10.1016/j.ygeno.2014.07.006 (2014).
- 12 Waterland, R. A. *et al.* Season of conception in rural Gambia affects DNA methylation at putative human metastable epialleles. *PLoS Genet.* **6**, e1001252, doi:10.1371/journal.pgen.1001252 (2010).

- 13 Esterhuysen, M. M., Linhart, H. G. & Kaufmann, S. H. Can the battle against tuberculosis gain from epigenetic research? *Trends Microbiol.* **20**, 220-226, doi:10.1016/j.tim.2012.03.002 (2012).
- 14 Sharma, G. *et al.* Genome-wide non-CpG methylation of the host genome during *M. tuberculosis* infection. *Sci. Rep.* **6**, 25006, doi:10.1038/srep25006 (2016).
- 15 Zheng, L. *et al.* Unraveling methylation changes of host macrophages in *Mycobacterium tuberculosis* infection. *Tuberculosis (Edinb)* **98**, 139-148, doi:10.1016/j.tube.2016.03.003 (2016).
- 16 Shell, S. S. *et al.* DNA methylation impacts gene expression and ensures hypoxic survival of *Mycobacterium tuberculosis*. *PLoS Pathog.* **9**, e1003419, doi:10.1371/journal.ppat.1003419 (2013).
- 17 Doherty, R. *et al.* The CD4(+) T cell methylome contributes to a distinct CD4(+) T cell transcriptional signature in *Mycobacterium bovis*-infected cattle. *Sci. Rep.* **6**, 31014, doi:10.1038/srep31014 (2016).
- 18 Marr, A. K. *et al.* *Leishmania donovani* infection causes distinct epigenetic DNA methylation changes in host macrophages. *PLoS Pathog.* **10**, e1004419, doi:10.1371/journal.ppat.1004419 (2014).
- 19 Sinclair, S. H., Yegnasubramanian, S. & Dumler, J. S. Global DNA methylation changes and differential gene expression in *Anaplasma phagocytophilum*-infected human neutrophils. *Clin. Epigenetics* **7**, 77, doi:10.1186/s13148-015-0105-1 (2015).
- 20 Sitaraman, R. *Helicobacter pylori* DNA methyltransferases and the epigenetic field effect in cancerization. *Front. Microbiol.* **5**, 115, doi:10.3389/fmicb.2014.00115 (2014).
- 21 Magee, D. A. *et al.* Innate cytokine profiling of bovine alveolar macrophages reveals commonalities and divergence in the response to *Mycobacterium bovis* and *Mycobacterium tuberculosis* infection. *Tuberculosis (Edinb)* **94**, 441-450, doi:10.1016/j.tube.2014.04.004 (2014).
- 22 Malone, K. M. *et al.* Comparative 'omics analyses differentiate *Mycobacterium tuberculosis* and *Mycobacterium bovis* and reveal distinct macrophage responses to infection with the human and bovine tubercle bacilli. *Microb. Genom.*, doi:10.1099/mgen.0.000163 (2018).
- 23 Nalpas, N. C. *et al.* RNA sequencing provides exquisite insight into the manipulation of the alveolar macrophage by tubercle bacilli. *Sci. Rep.* **5**, 13629, doi:10.1038/srep13629 (2015).

- 24 Vegh, P. *et al.* MicroRNA profiling of the bovine alveolar macrophage response to *Mycobacterium bovis* infection suggests pathogen survival is enhanced by microRNA regulation of endocytosis and lysosome trafficking. *Tuberculosis (Edinb)* **95**, 60-67 (2015).
- 25 O'Doherty, A. M. *et al.* DNA methylation dynamics at imprinted genes during bovine pre-implantation embryo development. *BMC Dev. Biol.* **15**, 13, doi:10.1186/s12861-015-0060-2 (2015).
- 26 O'Doherty, A. M. *et al.* DNA methylation plays an important role in promoter choice and protein production at the mouse *Dnmt3L* locus. *Dev. Biol.* **356**, 411-420, doi:10.1016/j.ydbio.2011.05.665 (2011).
- 27 O'Doherty, A. M., O'Shea, L. C. & Fair, T. Bovine DNA methylation imprints are established in an oocyte size-specific manner, which are coordinated with the expression of the DNMT3 family proteins. *Biol. Reprod.* **86**, 67, doi:10.1095/biolreprod.111.094946 (2012).
- 28 Krueger, F. & Andrews, S. R. Bismark: a flexible aligner and methylation caller for Bisulfite-Seq applications. *Bioinformatics* **27**, 1571-1572, doi:10.1093/bioinformatics/btr167 (2011).
- 29 Langmead, B. & Salzberg, S. L. Fast gapped-read alignment with Bowtie 2. *Nat. Methods* **9**, 357-359, doi:10.1038/nmeth.1923 (2012).
- 30 Zimin, A. V. *et al.* A whole-genome assembly of the domestic cow, *Bos taurus*. *Genome Biol.* **10**, R42, doi:10.1186/gb-2009-10-4-r42 (2009).
- 31 Hansen, K. D., Langmead, B. & Irizarry, R. A. BSmooth: from whole genome bisulfite sequencing reads to differentially methylated regions. *Genome Biol.* **13**, R83, doi:10.1186/gb-2012-13-10-r83 (2012).
- 32 Karolchik, D. *et al.* The UCSC Table Browser data retrieval tool. *Nucleic Acids Res.* **32**, D493-496, doi:10.1093/nar/gkh103 (2004).
- 33 Akalin, A. *et al.* methylKit: a comprehensive R package for the analysis of genome-wide DNA methylation profiles. *Genome Biol.* **13**, R87, doi:10.1186/gb-2012-13-10-r87 (2012).
- 34 Benjamini, Y. & Hochberg, Y. Controlling the false discovery rate - a practical and powerful approach to multiple testing. *J. R. Stat. Soc. Ser. B Method.* **57**, 289-300 (1995).

- 35 Young, M. D., Wakefield, M. J., Smyth, G. K. & Oshlack, A. Gene ontology analysis for RNA-seq: accounting for selection bias. *Genome Biol.* **11**, R14, doi:10.1186/gb-2010-11-2-r14 (2010).
- 36 Ziller, M. J., Hansen, K. D., Meissner, A. & Aryee, M. J. Coverage recommendations for methylation analysis by whole-genome bisulfite sequencing. *Nat. Methods* **12**, 230-232, doi:10.1038/nmeth.3152 (2015).
- 37 Clark, S. J. *et al.* Genome-wide base-resolution mapping of DNA methylation in single cells using single-cell bisulfite sequencing (scBS-seq). *Nat. Protoc.* **12**, 534-547, doi:10.1038/nprot.2016.187 (2017).
- 38 Peat, J. R. *et al.* Genome-wide bisulfite sequencing in zygotes identifies demethylation targets and maps the contribution of TET3 oxidation. *Cell Rep.* **9**, 1990-2000, doi:10.1016/j.celrep.2014.11.034 (2014).
- 39 Chen, Z. X. & Riggs, A. D. DNA methylation and demethylation in mammals. *J. Biol. Chem.* **286**, 18347-18353, doi:10.1074/jbc.R110.205286 (2011).
- 40 Deaton, A. M. *et al.* Cell type-specific DNA methylation at intragenic CpG islands in the immune system. *Genome Res.* **21**, 1074-1086, doi:10.1101/gr.118703.110 (2011).
- 41 Elliott, G. *et al.* Intermediate DNA methylation is a conserved signature of genome regulation. *Nat. Commun.* **6**, 6363, doi:10.1038/ncomms7363 (2015).
- 42 Nestorov, P., Hotz, H. R., Liu, Z. & Peters, A. H. Dynamic expression of chromatin modifiers during developmental transitions in mouse preimplantation embryos. *Sci. Rep.* **5**, 14347, doi:10.1038/srep14347 (2015).
- 43 Smith, Z. D. & Meissner, A. DNA methylation: roles in mammalian development. *Nat. Rev. Genet.* **14**, 204-220, doi:10.1038/nrg3354 (2013).
- 44 Jones, P. A. Functions of DNA methylation: islands, start sites, gene bodies and beyond. *Nat. Rev. Genet.* **13**, 484-492, doi:10.1038/nrg3230 (2012).
- 45 Lyu, L. N., Jia, H. Y., Li, Z. H., Liu, Z. Q. & Zhang, Z. D. [Changes and differences of DNA methylation in human macrophages infected with virulent and avirulent *Mycobacterium tuberculosis*]. *Zhonghua Jie He He Hu Xi Za Zhi* **40**, 509-514, doi:10.3760/cma.j.issn.1001-0939.2017.07.006 (2017).
- 46 Sharma, G., Upadhyay, S., Srilalitha, M., Nandicoori, V. K. & Khosla, S. The interaction of mycobacterial protein Rv2966c with host chromatin is mediated through non-CpG methylation and histone H3/H4 binding. *Nucleic Acids Res.* **43**, 3922-3937, doi:10.1093/nar/gkv261 (2015).

- 47 Yaseen, I., Kaur, P., Nandicoori, V. K. & Khosla, S. Mycobacteria modulate host epigenetic machinery by Rv1988 methylation of a non-tail arginine of histone H3. *Nat. Commun.* **6**, 8922, doi:10.1038/ncomms9922 (2015).
- 48 Weber, M. *et al.* Distribution, silencing potential and evolutionary impact of promoter DNA methylation in the human genome. *Nat. Genet.* **39**, 457-466, doi:10.1038/ng1990 (2007).
- 49 Pervjakova, N. *et al.* Imprinted genes and imprinting control regions show predominant intermediate methylation in adult somatic tissues. *Epigenomics* **8**, 789-799, doi:10.2217/epi.16.8 (2016).
- 50 Andersson, L. *et al.* Coordinated international action to accelerate genome-to-phenome with FAANG, the Functional Annotation of Animal Genomes project. *Genome Biol.* **16**, 57, doi:10.1186/s13059-015-0622-4 (2015).
- 51 Edgar, R., Domrachev, M. & Lash, A. E. Gene Expression Omnibus: NCBI gene expression and hybridization array data repository. *Nucleic Acids Res.* **30**, 207-210 (2002).



Wash and seed
Alveolar macrophages



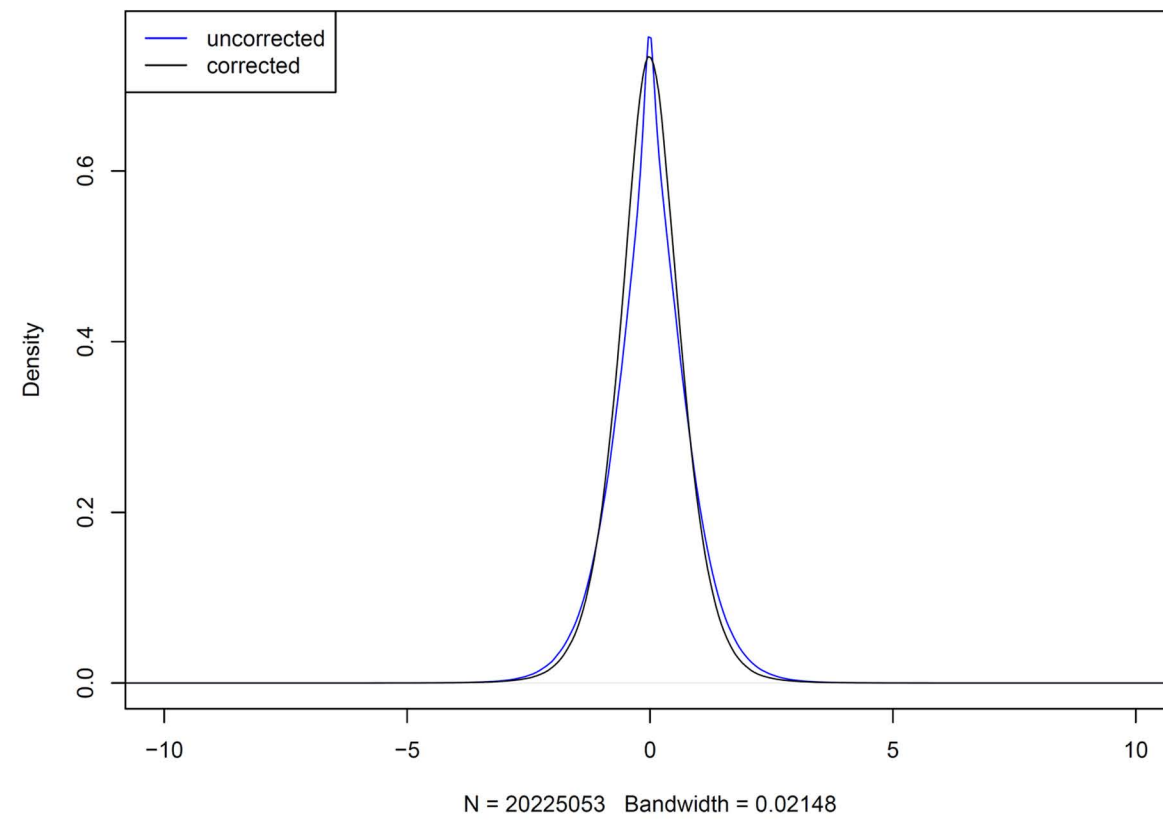
Control

M. bovis

Whole Genome
Bisulfite Sequencing

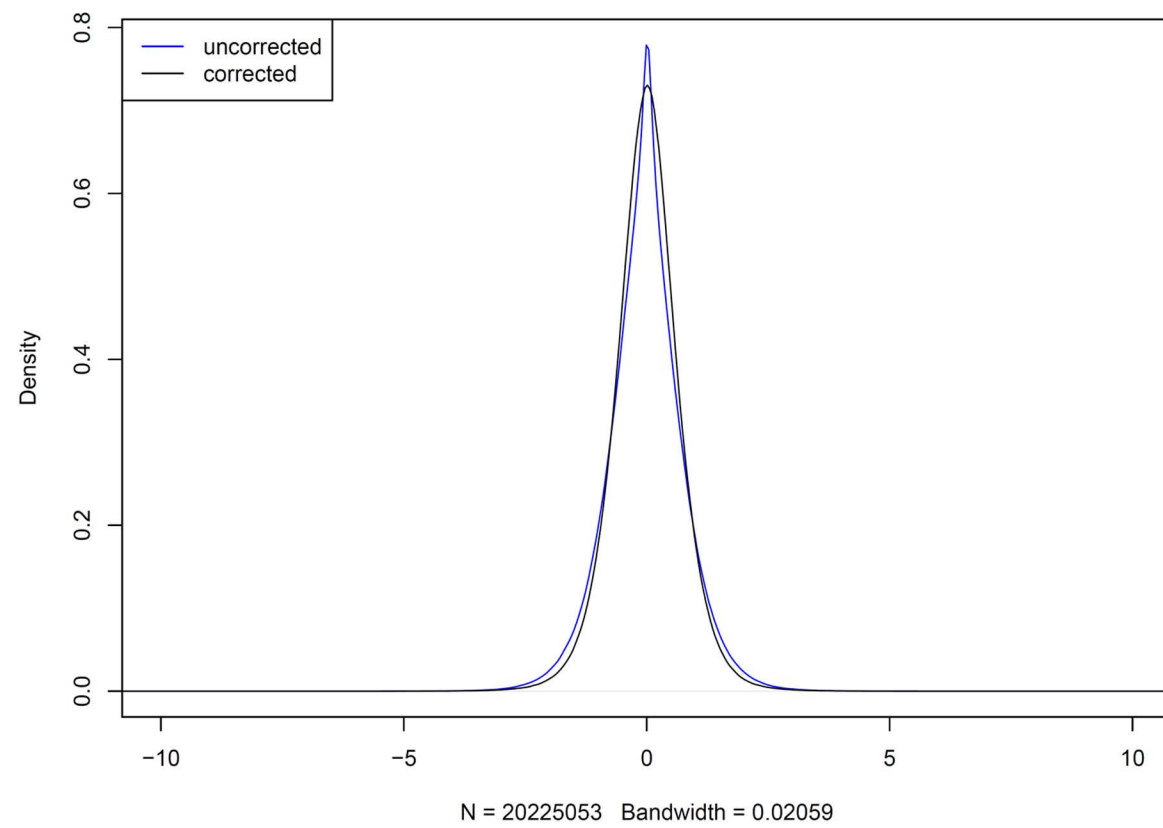
Pyrosequencing

Distribution of t -statistics

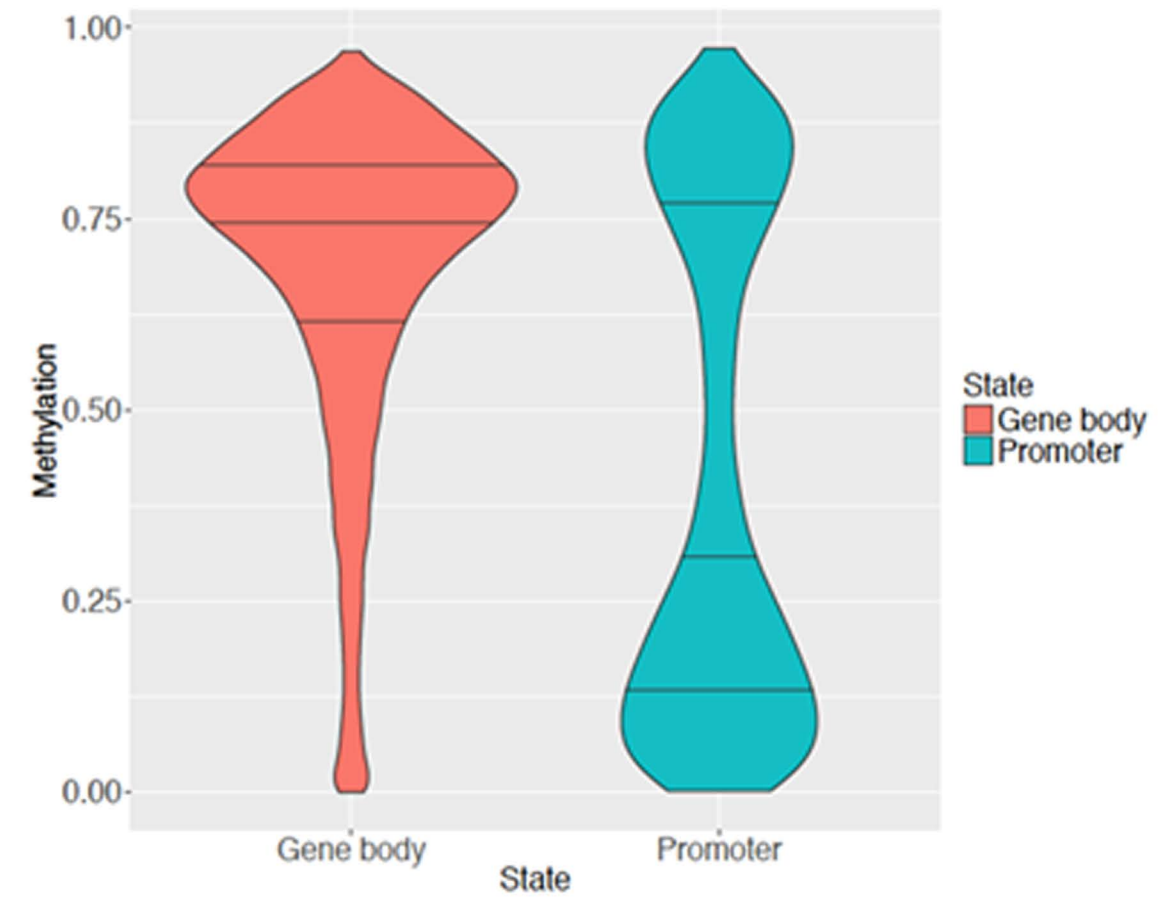


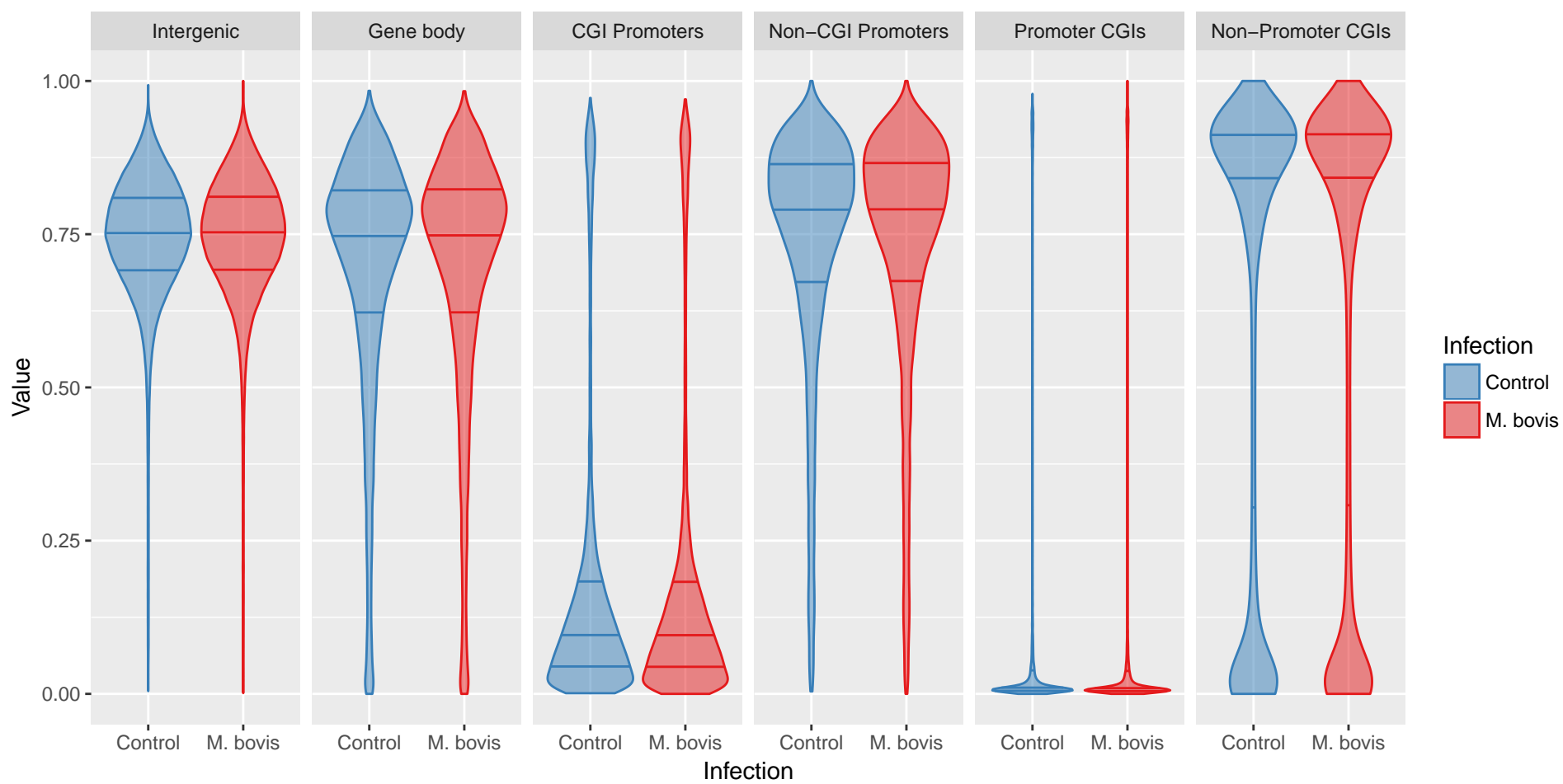
B

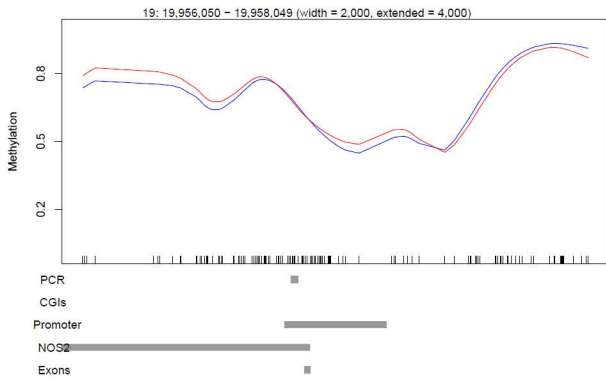
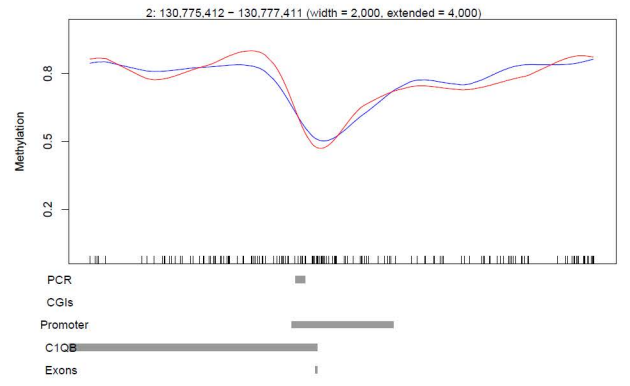
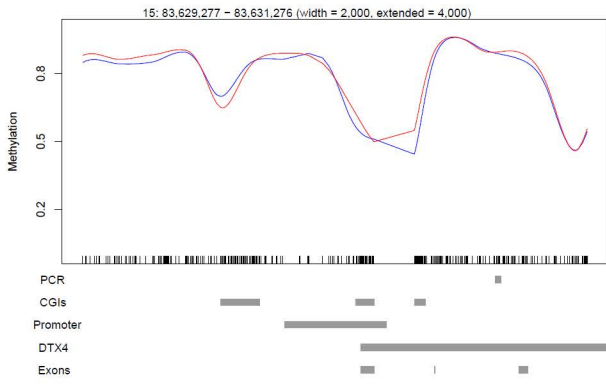
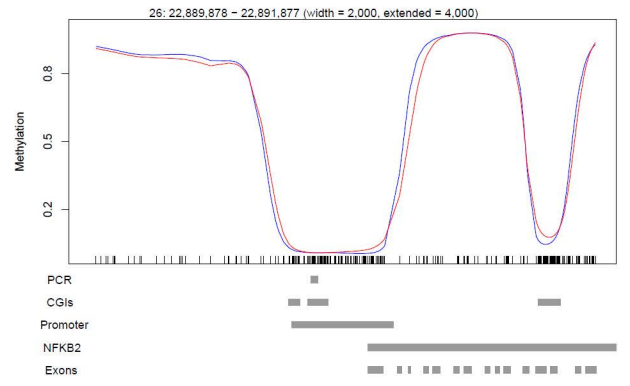
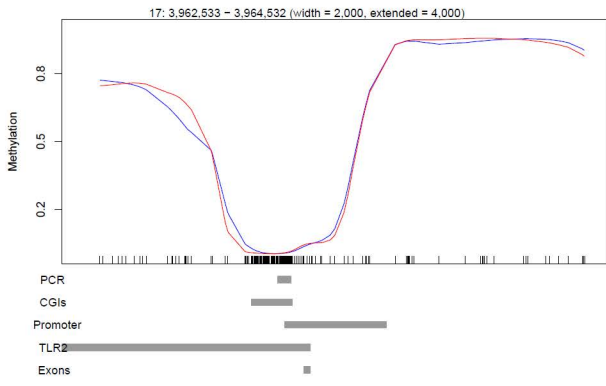
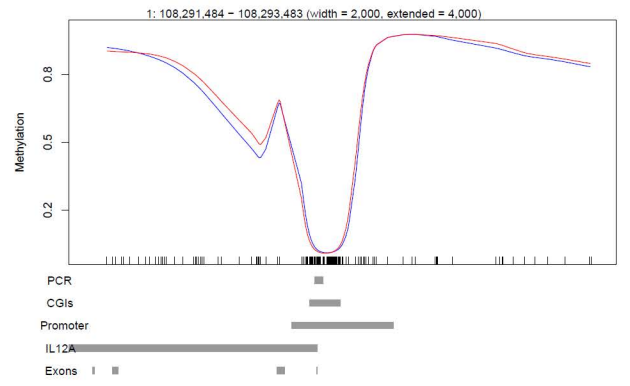
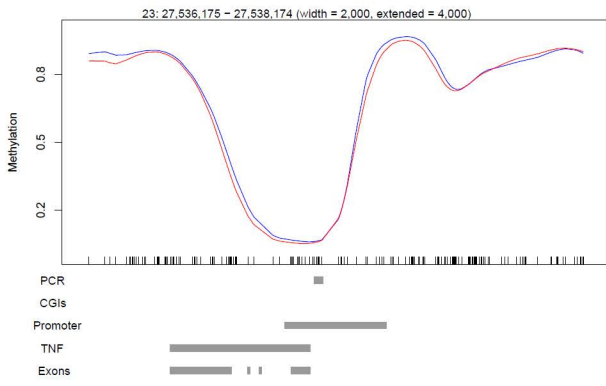
Randomised samples

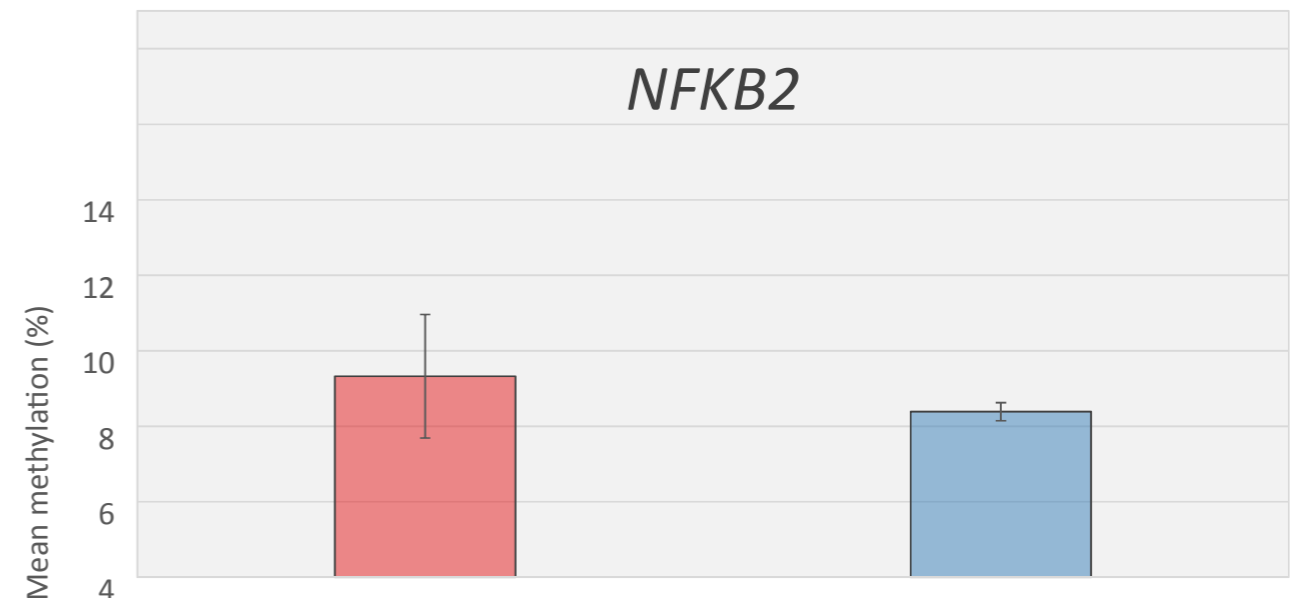
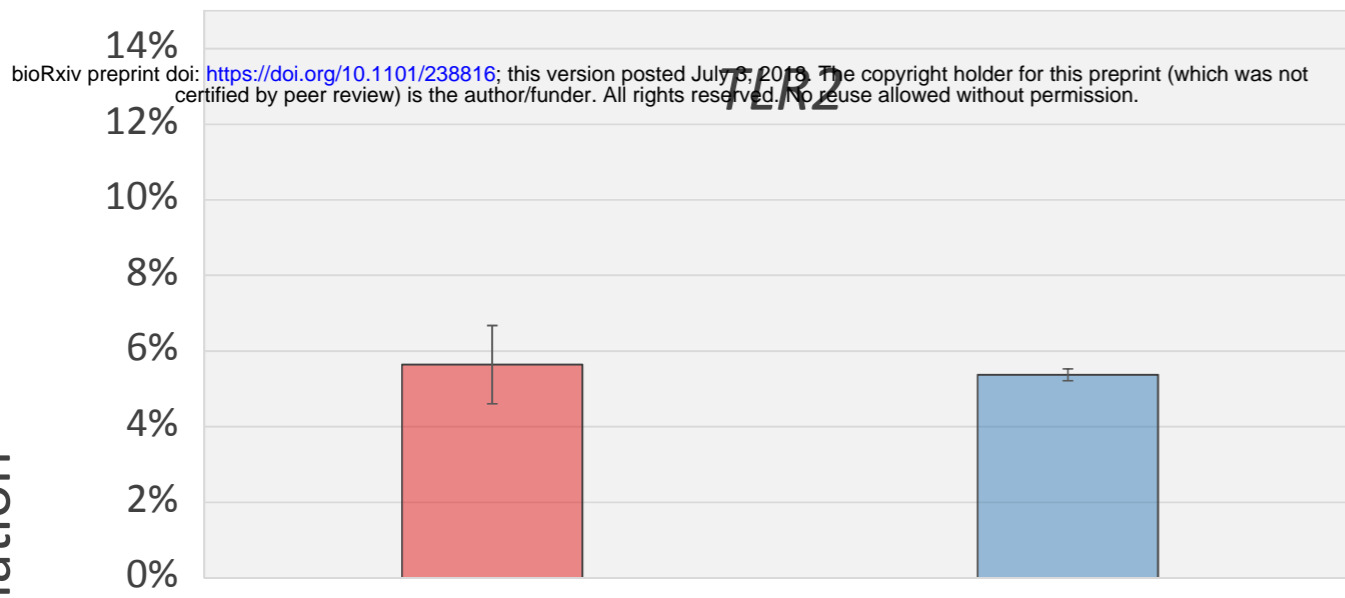
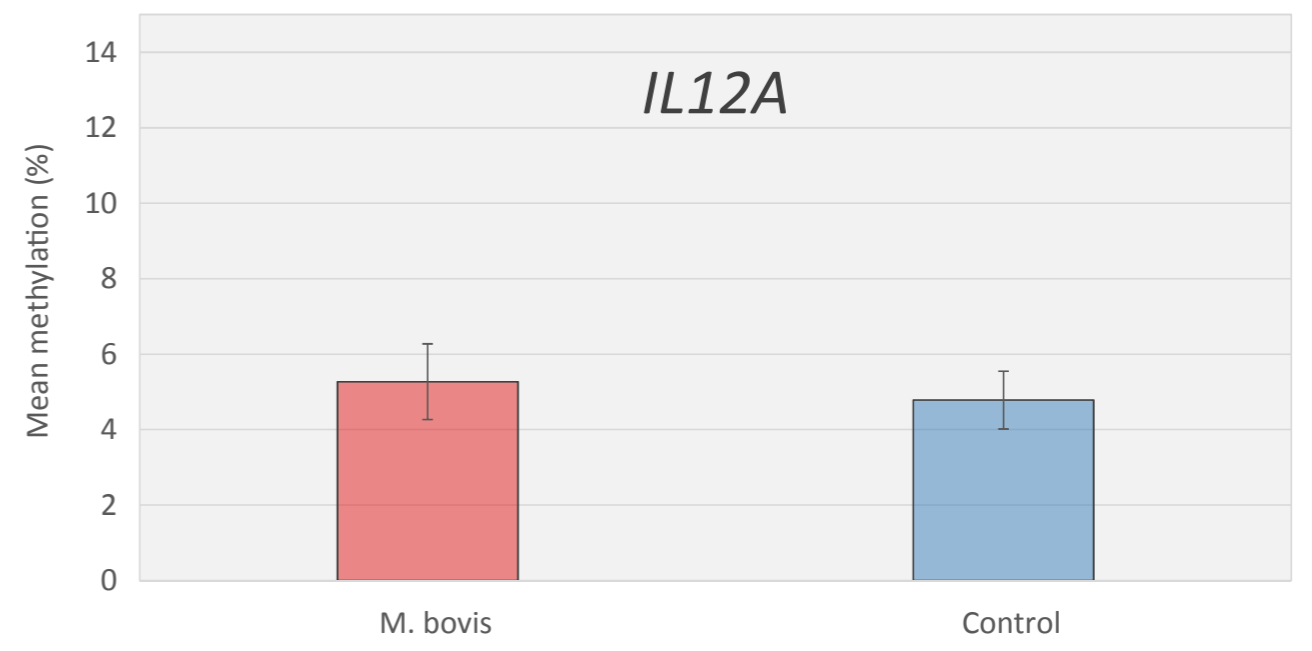
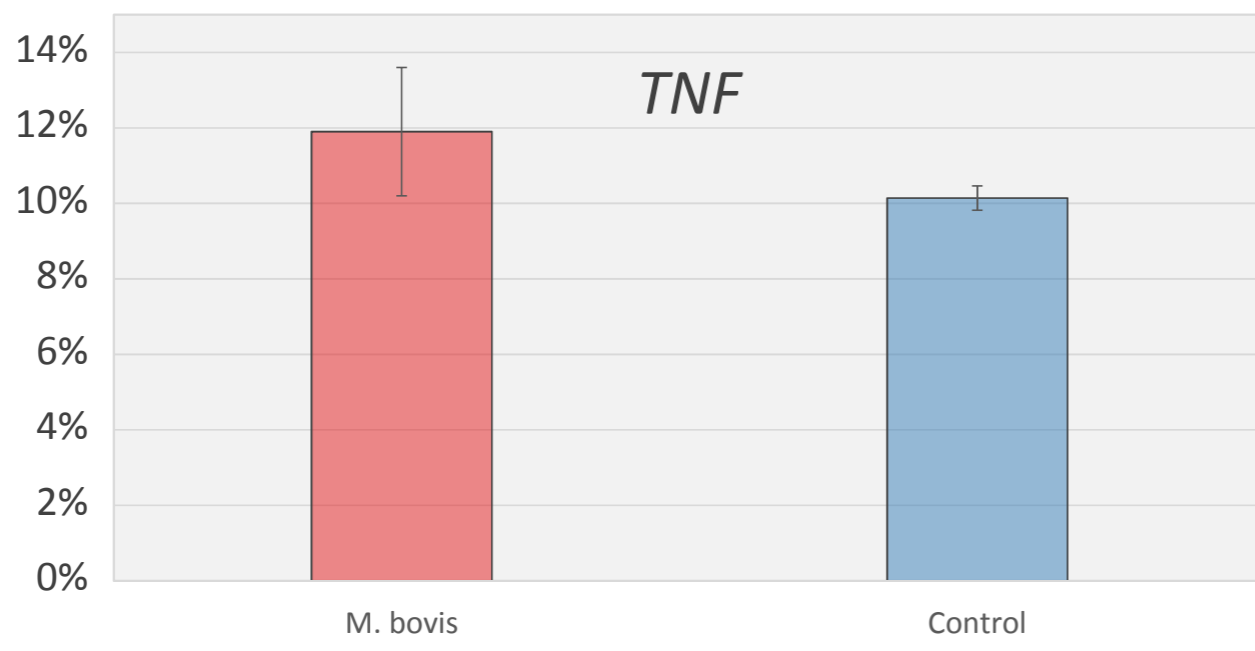


C

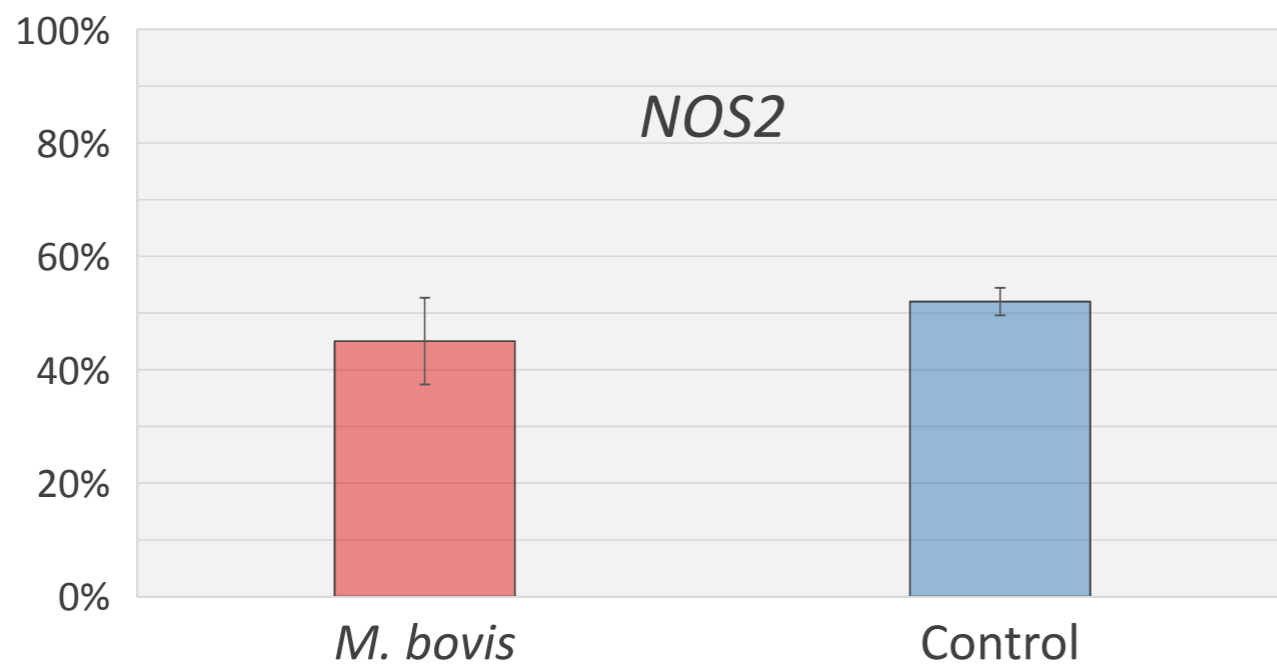
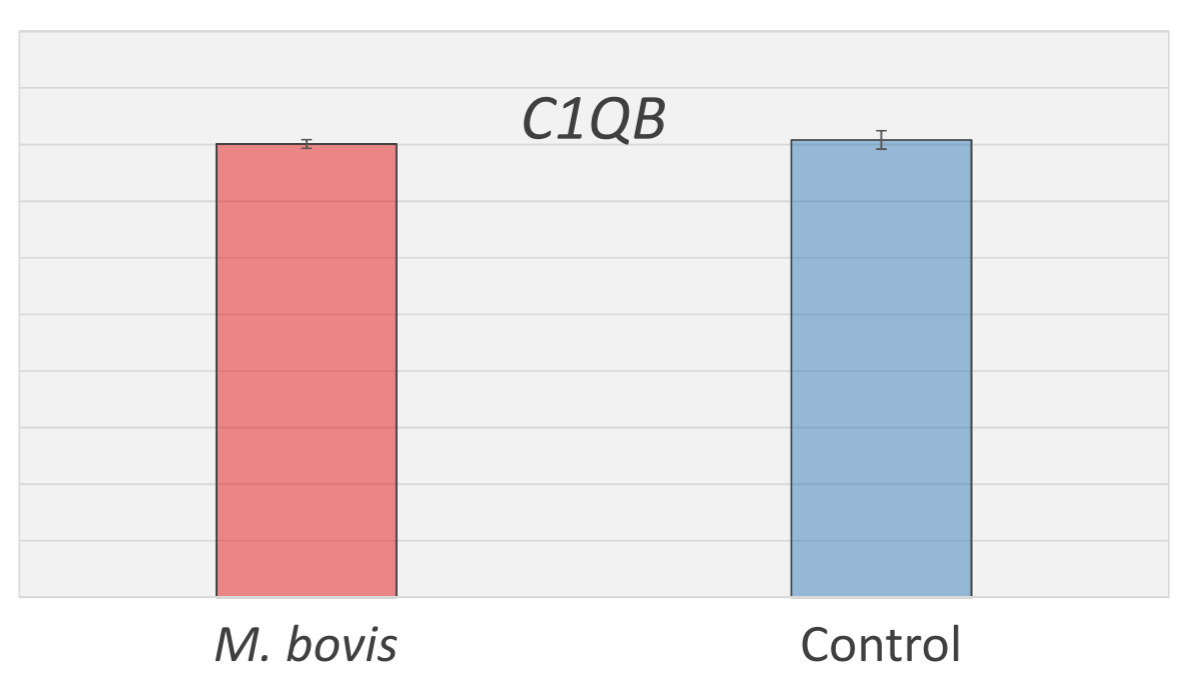
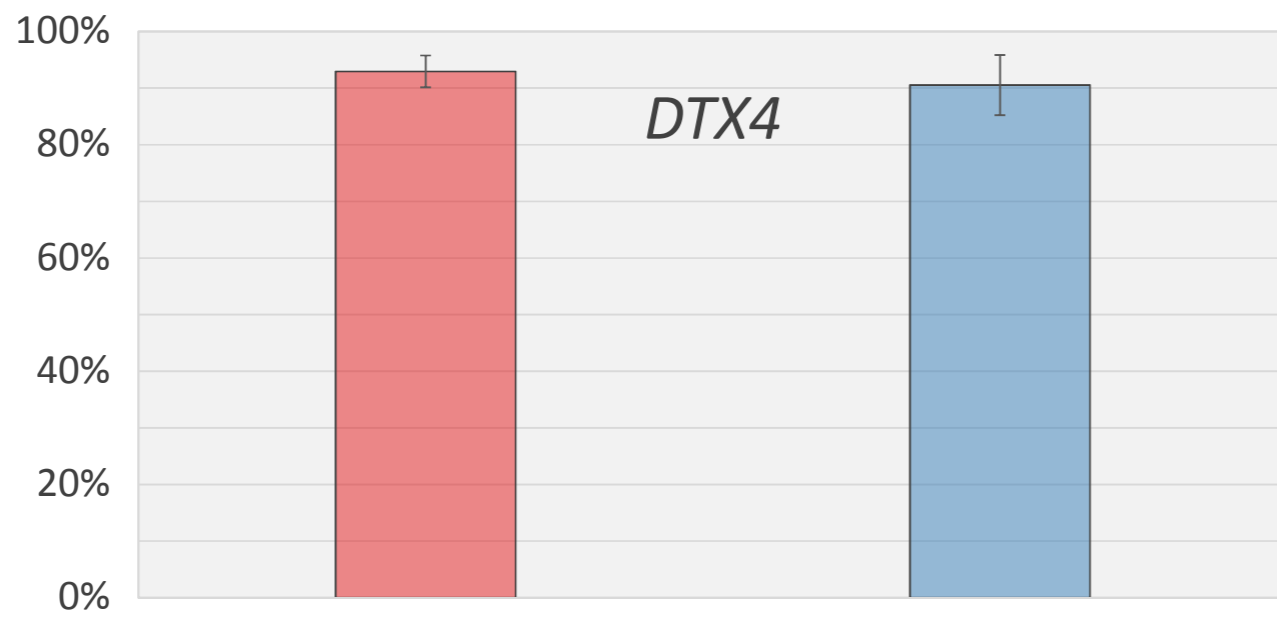






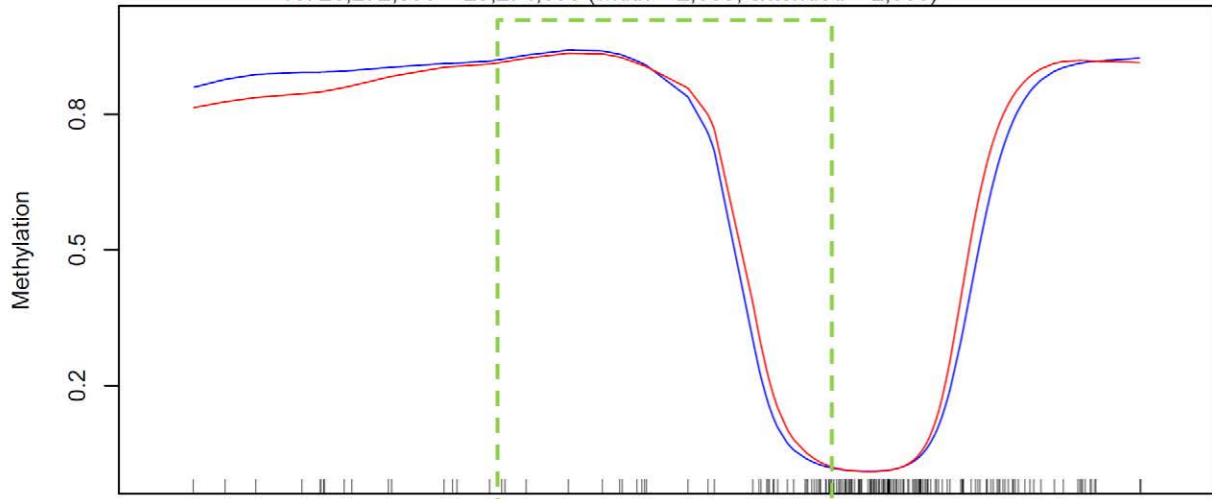


Mean methylation



bioRxiv preprint doi: <https://doi.org/10.1101/238816>; this version posted July 3, 2019. The copyright holder for this preprint (which was not certified by peer review) is the author/funder. All rights reserved. No reuse allowed without permission.

19: 28,272,599 – 28,274,598 (width = 2,000, extended = 2,000)

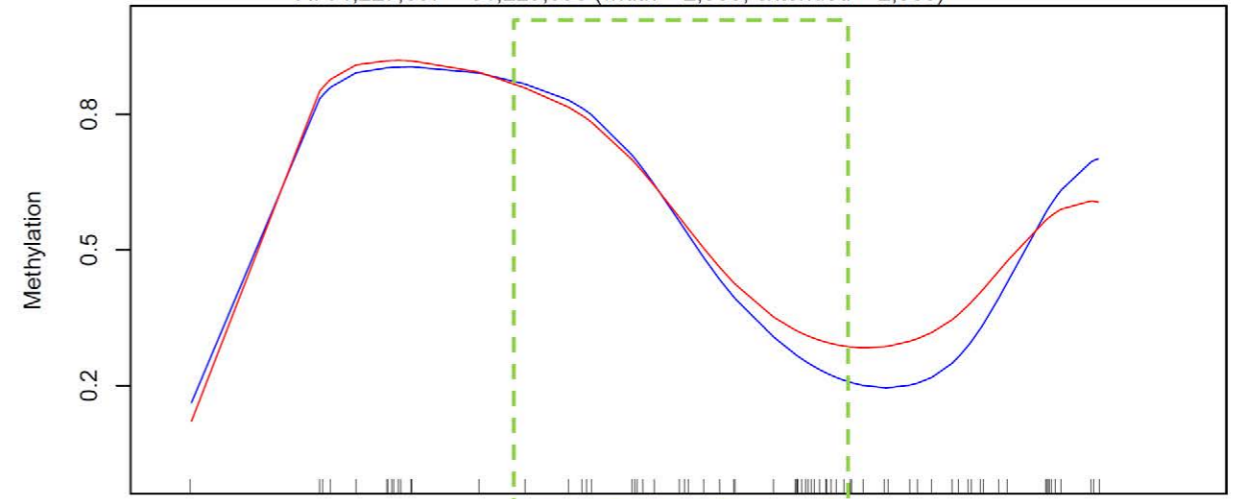


Promoter

GUCY2D

Exons

X: 91,227,557 – 91,229,556 (width = 2,000, extended = 2,000)

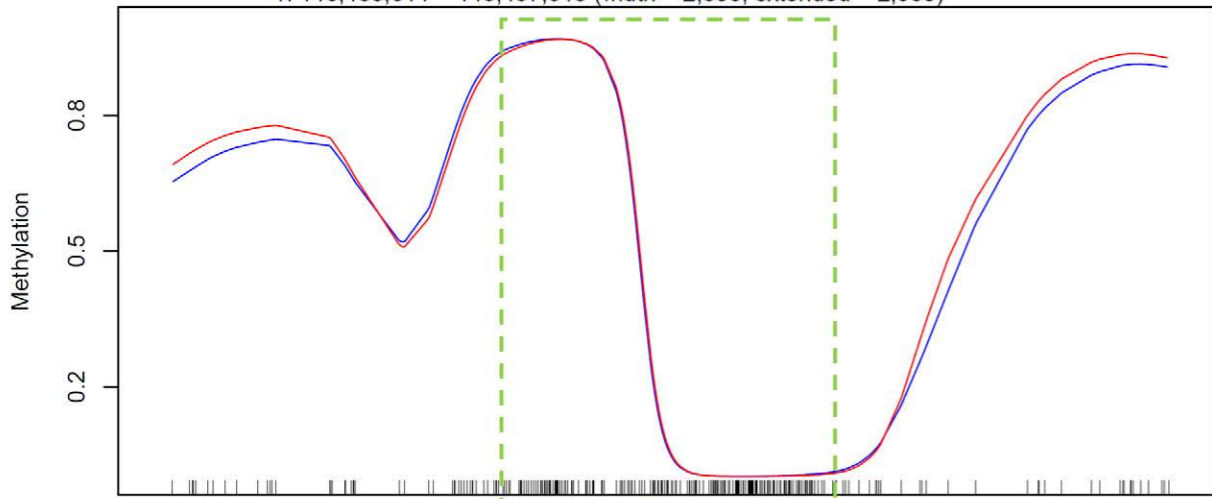


Promoter

SYN1

Exons

1: 146,435,614 – 146,437,613 (width = 2,000, extended = 2,000)

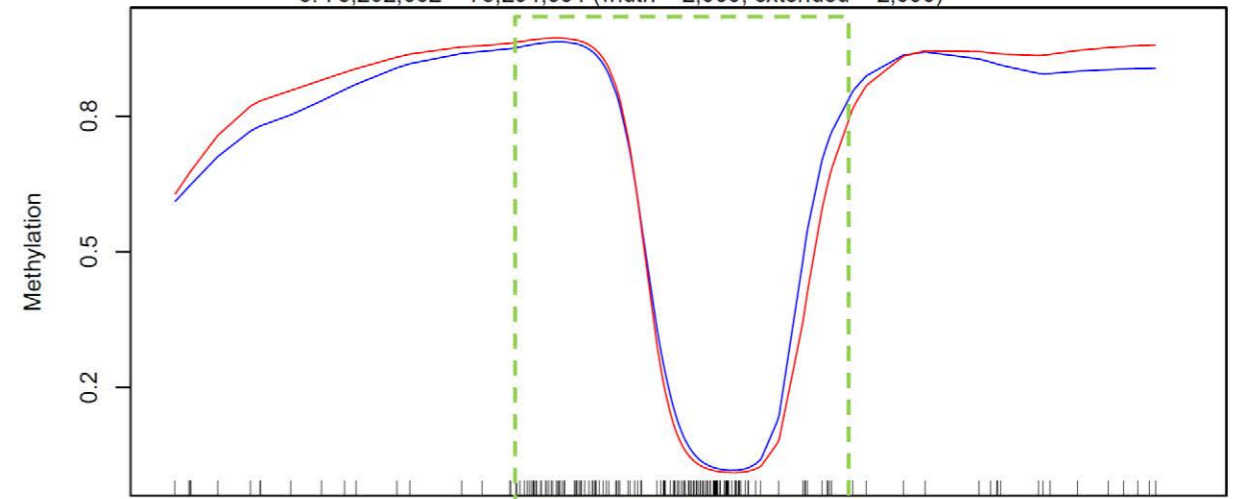


Promoter

RRP1B

Exons

5: 75,292,002 – 75,294,001 (width = 2,000, extended = 2,000)

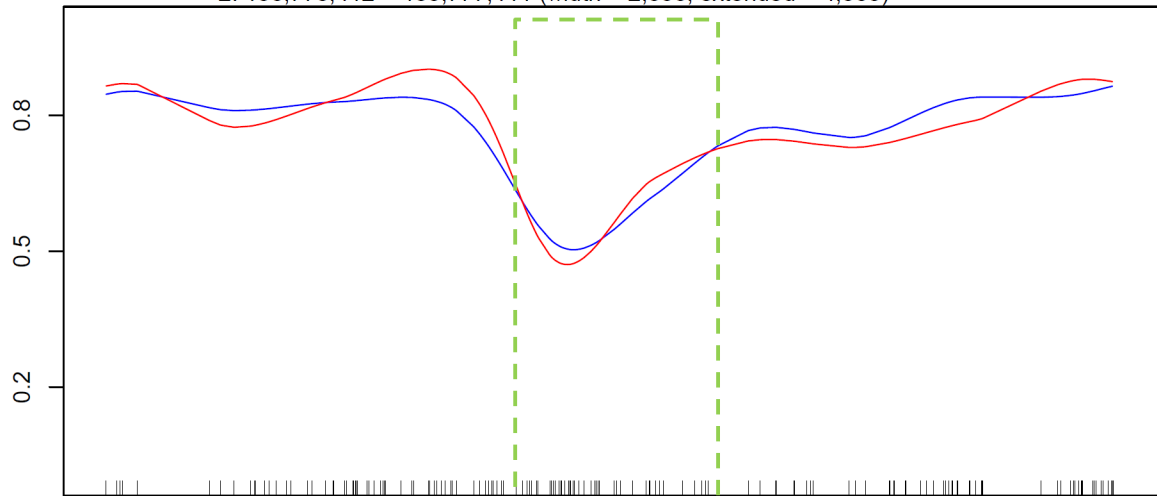


Promoter

FOXRED2

Exons

2: 130,775,412 - 130,777,411 (width = 2,000, extended = 4,000)



PCR

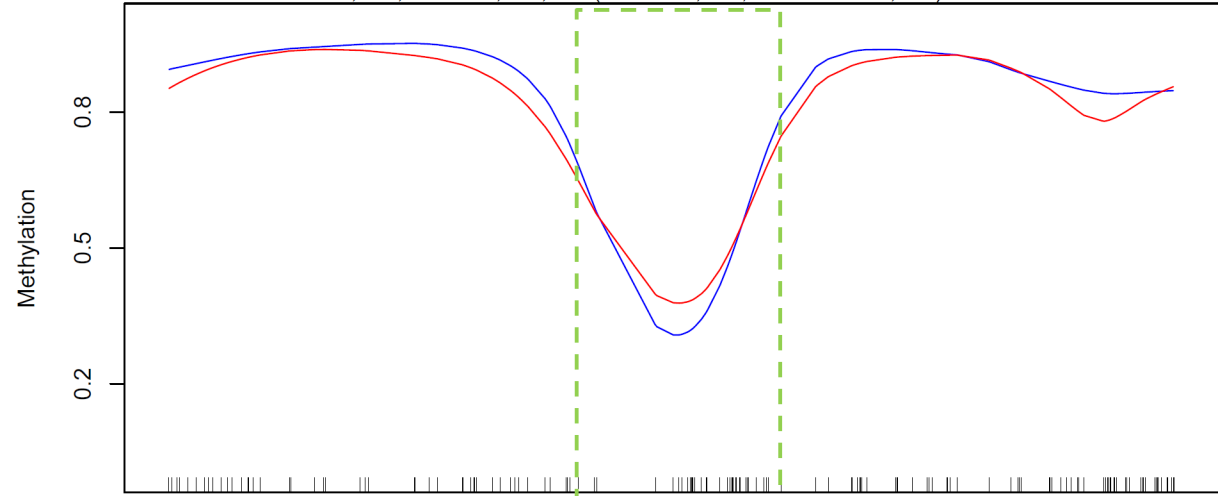
CGIs

C1QB

Gene

Exons

13: 17,539,461 - 17,541,460 (width = 2,000, extended = 4,000)



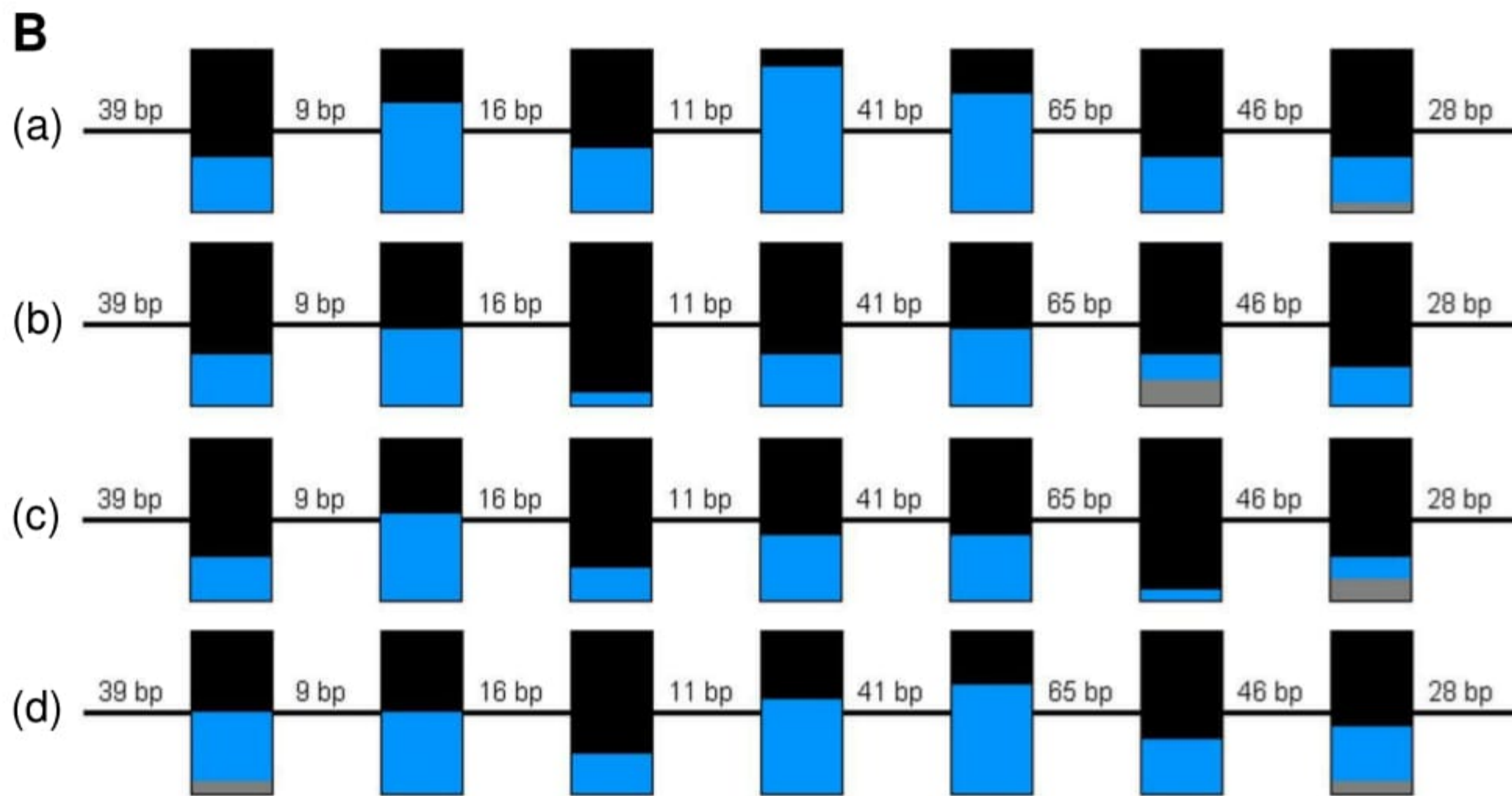
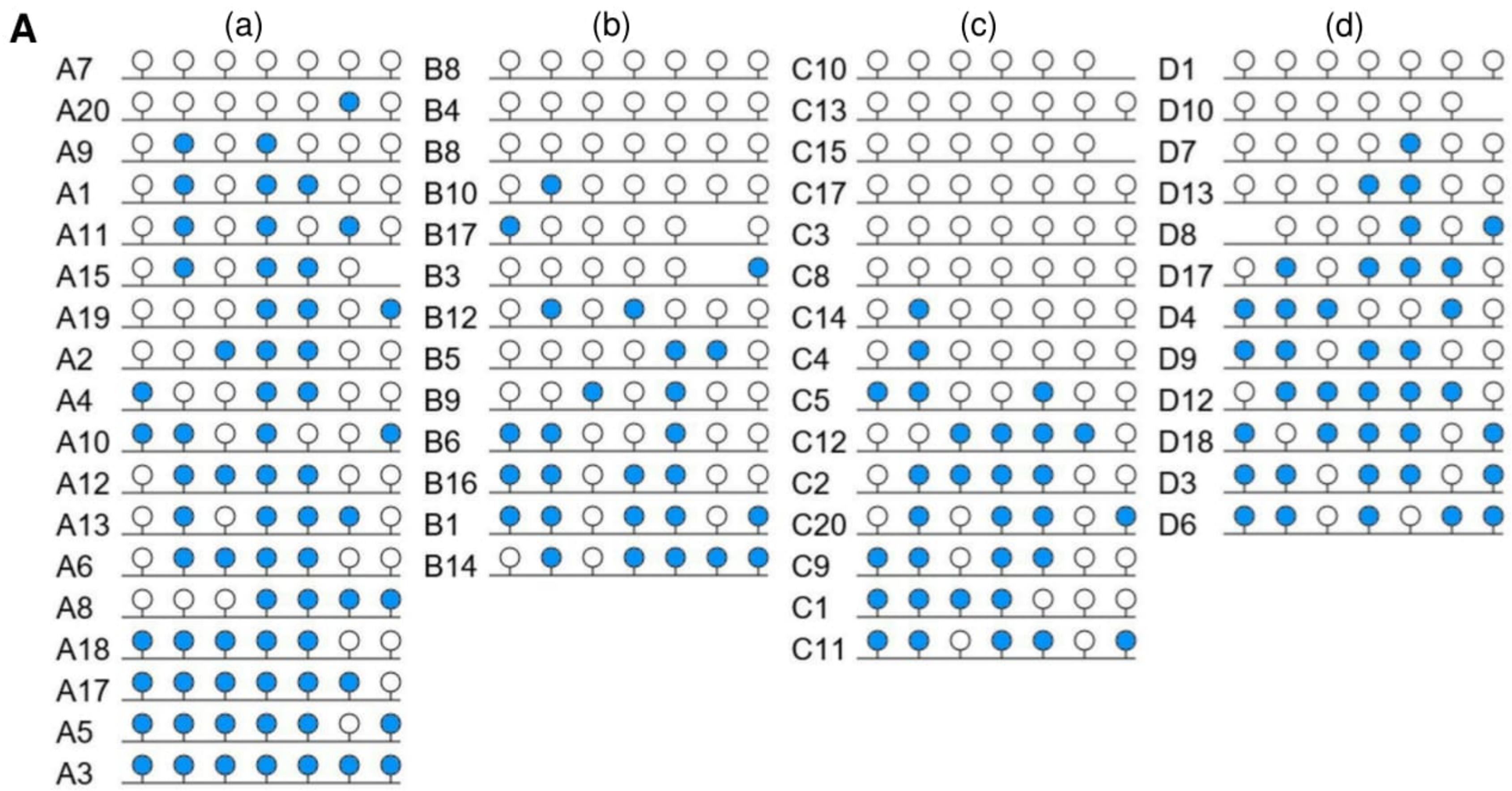
PCR

CGIs

IL2RA

Gene

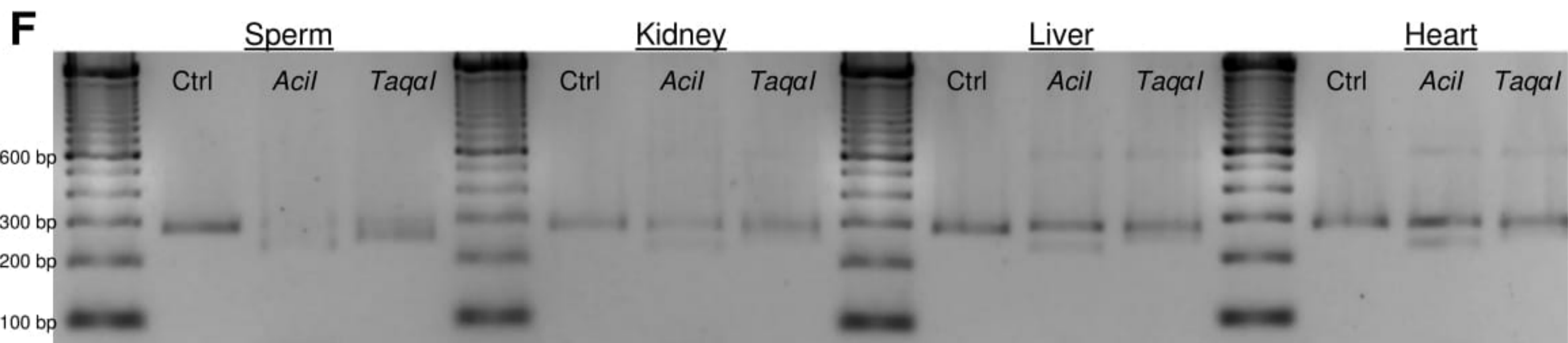
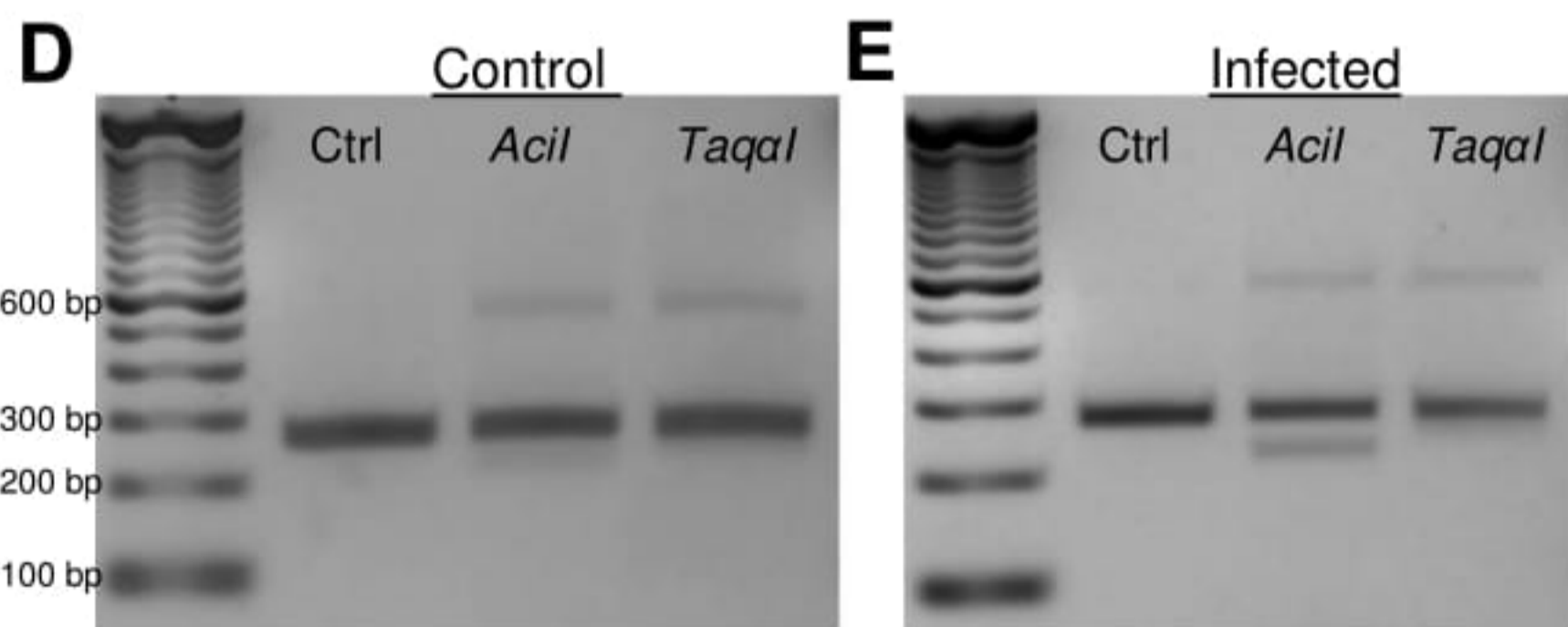
Exons

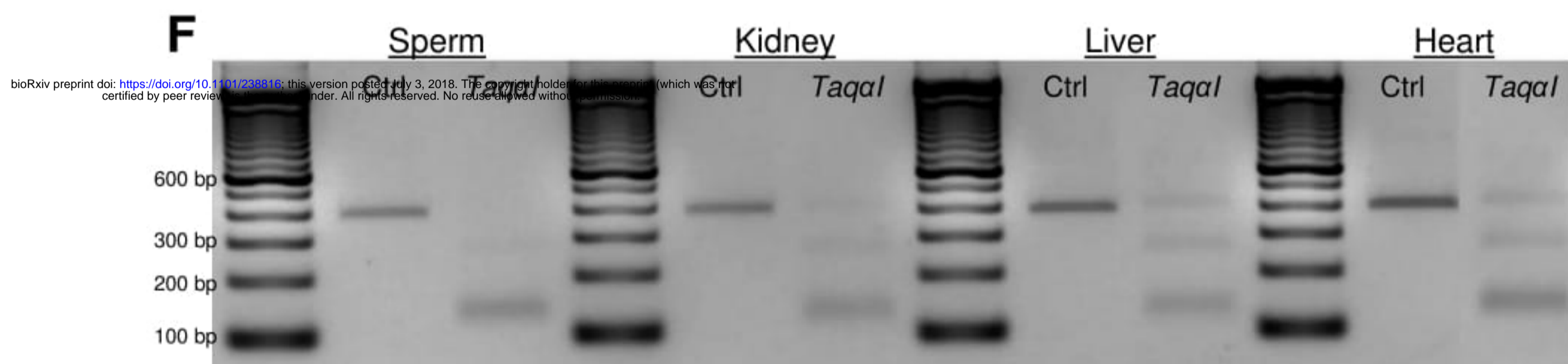
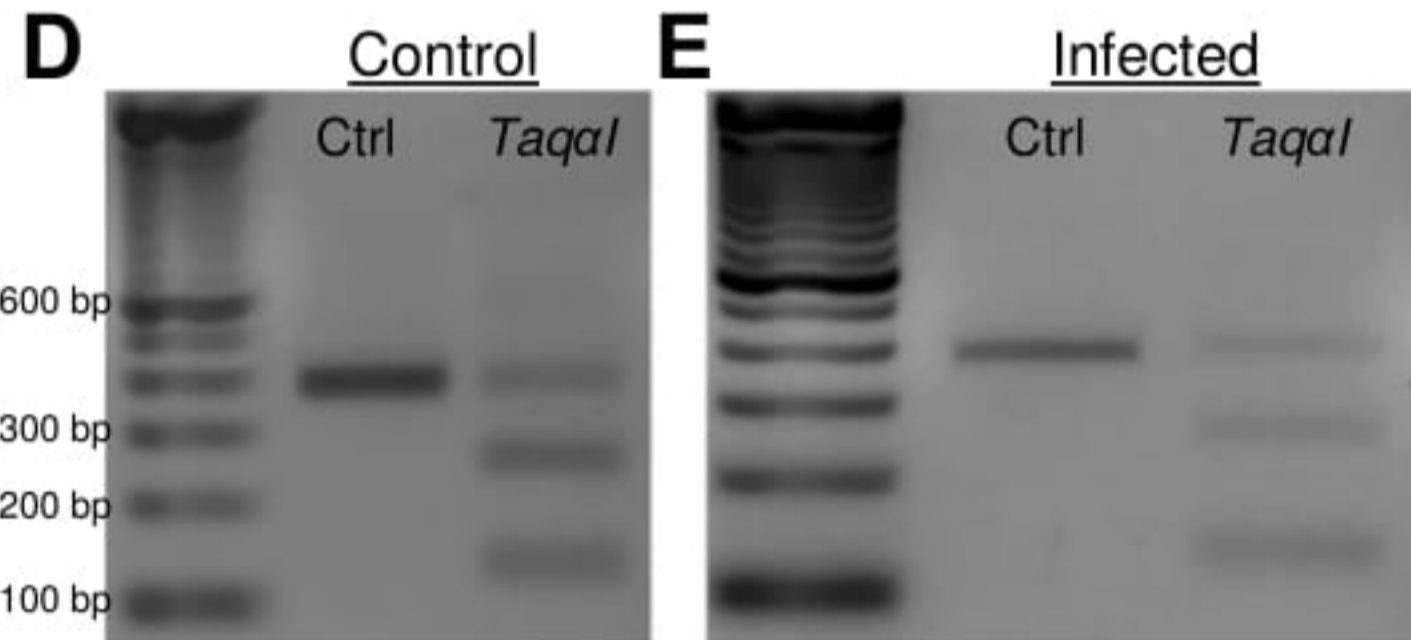
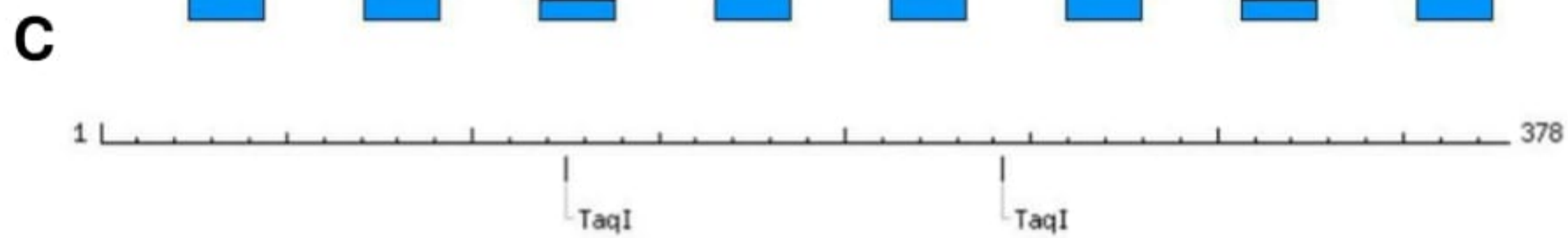
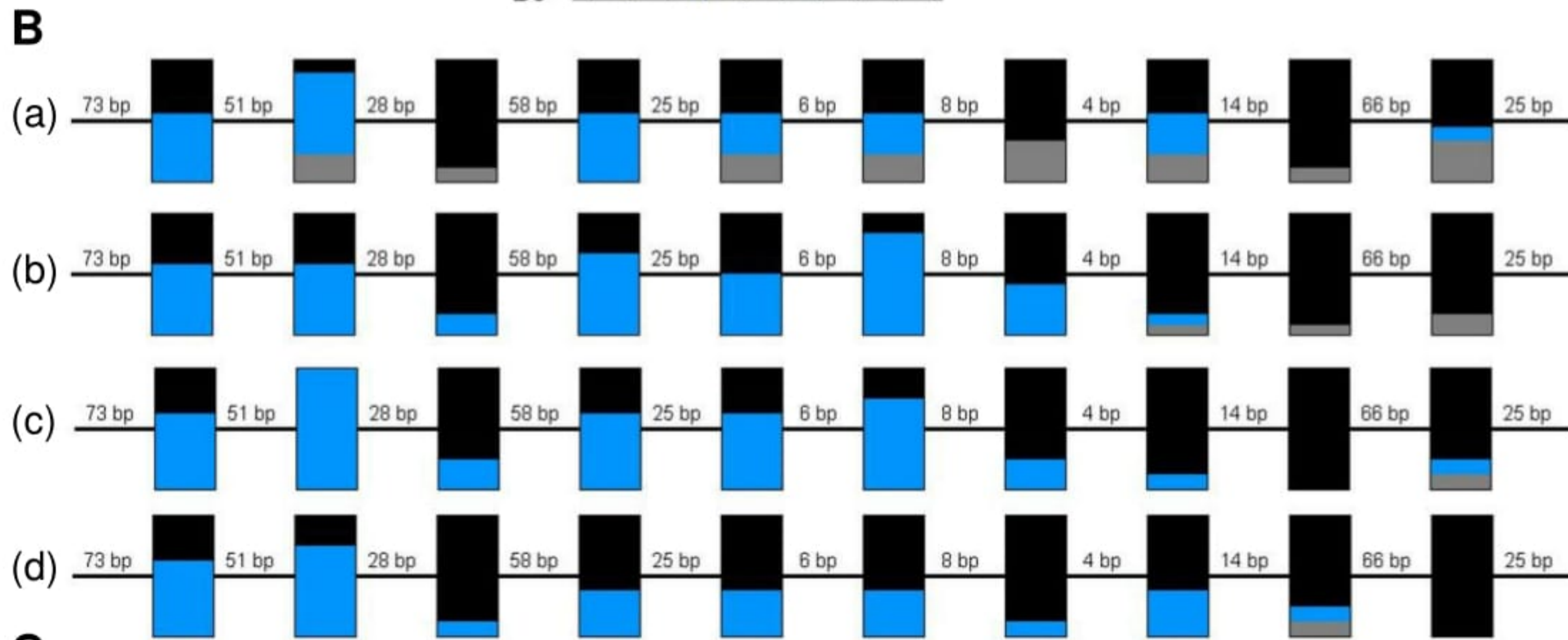
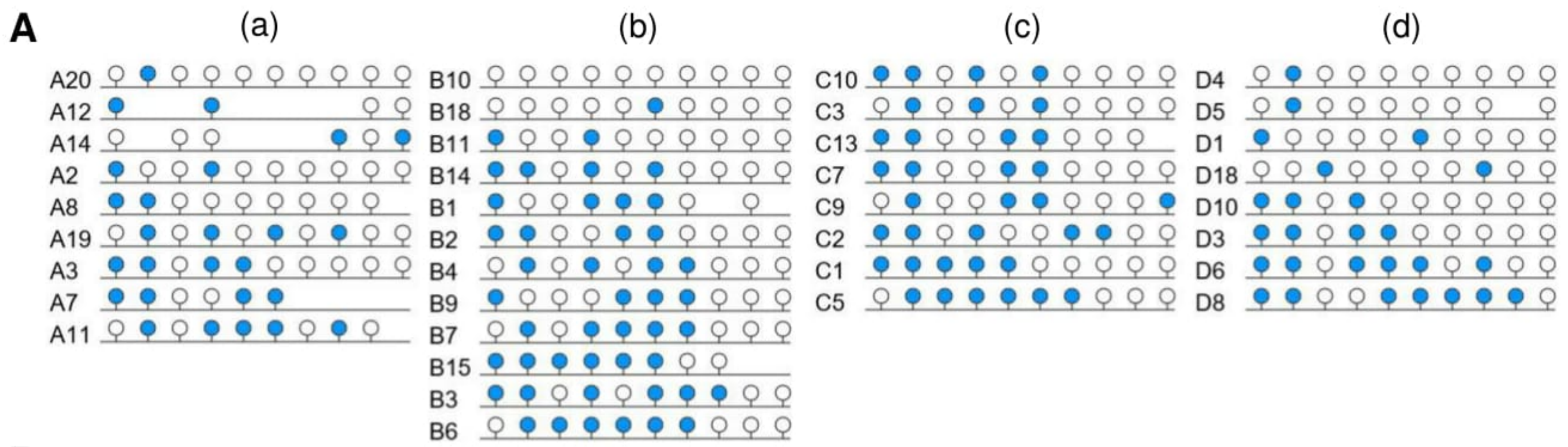


C

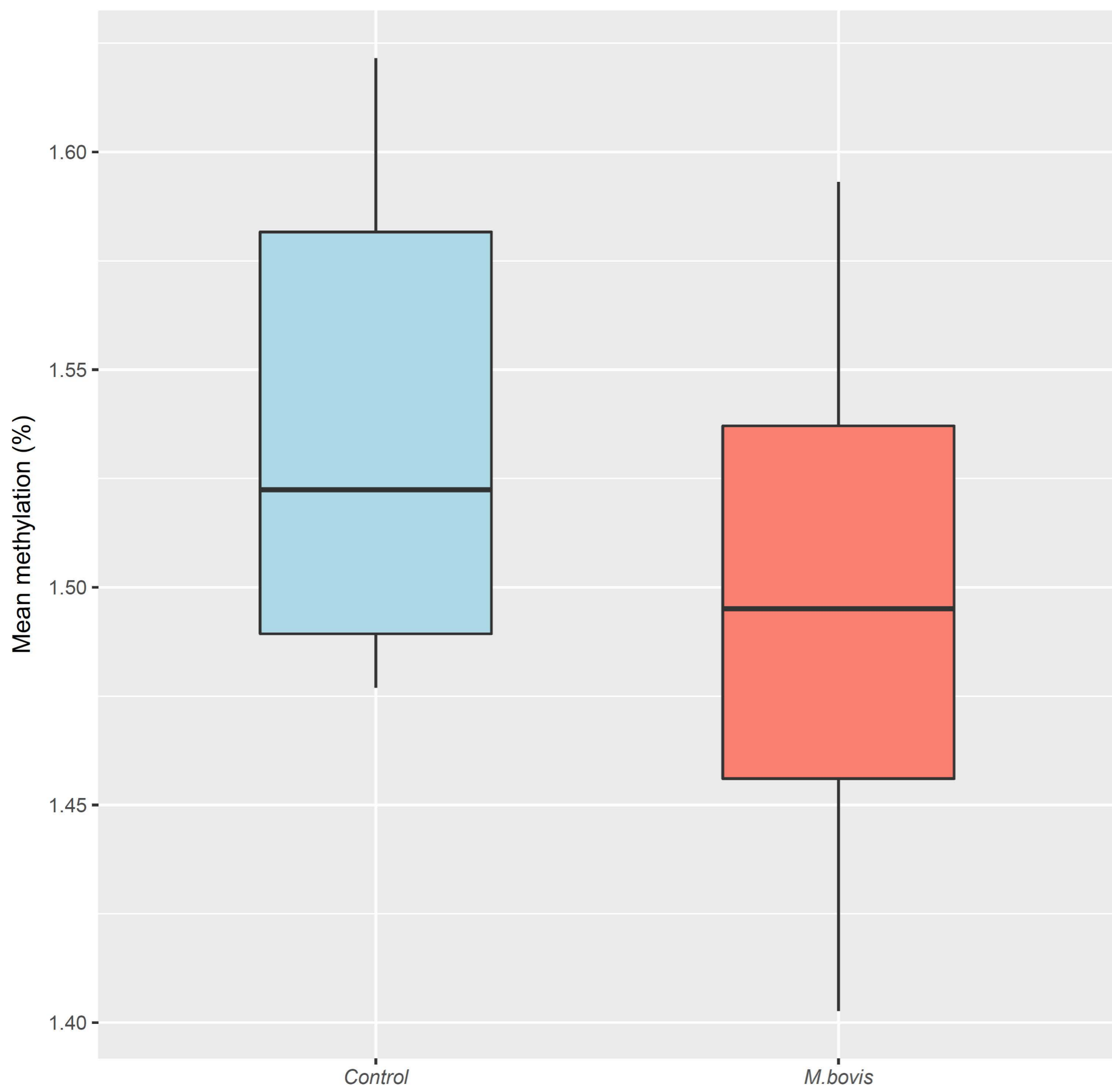
bioRxiv preprint doi: <https://doi.org/10.1101/338816>; this version posted July 3, 2018. The copyright holder for this preprint (which was not certified by peer review) is the author/funder. All rights reserved. No reuse allowed without permission.

AcII TaqI





CHG



CHH

